UNIVERSIDADE ESTADUAL DE CAMPINAS

FACULDADE DE CIÊNCIAS MÉDICAS

PAULO AFONSO MEI

ANÁLISE DE LESÕES ENCEFÁLICAS DE NATUREZAS DIFERENTES EM IMAGENS DE RESSONÂNCIA MAGNÉTICA E TOMOGRAFIA COMPUTADORIZADA A PARTIR DE MAPAS AUTO-ORGANIZÁVEIS

ANALYSIS OF ENCEPHALIC LESIONS OF DIFFERENT NATURES IN MAGNETIC RESONANCE AND COMPUTED TOMOGRAPHY IMAGES BY SELF ORGANIZING MAPS

CAMPINAS

2018

PAULO AFONSO MEI

ANÁLISE DE LESÕES ENCEFÁLICAS DE NATUREZAS DIFERENTES EM IMAGENS DE RESSONÂNCIA MAGNÉTICA E TOMOGRAFIA COMPUTADORIZADA A PARTIR DE MAPAS AUTO-ORGANIZÁVEIS

ANALISIS OF ENCEPHALIC LESIONS OF DIFFERENT NATURES IN MAGNETIC RESSONANCE AND COMPUTED TOMOGRAPHY IMAGES FROM SELF ORGANIZING MAPS

Tese apresentada à Faculdade de Ciências Médicas da Universidade Estadual de Campinas como parte dos requisitos exigidos para a obtenção do título de Doutor em Ciências, área de concentração Neurologia

Thesis presented to the Faculty of Medical Sciences of University of Campinas as part of the pre-requisites demanded for the obtention of the PhD degree in Medical Sciences, in the concentration area of Neurology

ORIENTADOR: Prof. Dr. Fabiano Reis
COORIENTADOR: Prof. Dr. Li Li Min

ESTE EXEMPLAR CORRESPONDE À VERSÃO
PARA A BANCA EXAMINADORA DA TESE DEFENDIDA PELO
ALUNO PAULO AFONSO MEI E ORIENTADA PELO
PROF. DR. FABIANO REIS.

CAMPINAS

2018

Agência(s) de fomento e nº(s) de processo(s): CAPES, 88881.132052/2016-01
ORCID: https://orcid.org/0000-0002-5484-228

Ficha catalográfica
Universidade Estadual de Campinas
Biblioteca da Faculdade de Ciências Médicas
Maristella Soares dos Santos - CRB 8/8402

Mei, Paulo Afonso, 1982-
M475a Análise de lesões encefálicas de naturezas diferentes em imagens de ressonância magnética e tomografia computadorizada a partir de mapas auto-organizáveis / Paulo Afonso Mei. – Campinas, SP : [s.n.], 2018.

Orientador: Fabiano Reis.
Coorientador: Li Li Min.
Tese (doutorado) – Universidade Estadual de Campinas, Faculdade de Ciências Médicas.

1. Mapas auto-organizáveis. 2. Ressonância magnética. 3. Redes neurais (Computação). 4. Tomografia computadorizada. 5. Segmentação de imagens médicas. I. Reis, Fabiano, 1975-. II. Li, Li Min, 1964-. III. Universidade Estadual de Campinas. Faculdade de Ciências Médicas. IV. Título.

Informações para Biblioteca Digital

Título em outro idioma: Analysis of encephalic lesions of different natures in magnetic resonance and computed tomography images from self-organizing maps
Palavras-chave em inglês:
Self-organizing maps
Magnetic resonance
Neural networks (Computer science)
Computed tomography
Medical image segmentation
Área de concentração: Neurologia
Titulação: Doutor em Ciências
Banca examinadora:
Fabiano Reis [Orientador]
Celso Darío Ramos
Claudia da Costa Leite
Diana Rodrigues de Pina Miranda
Tânia Aparecida Marchiori de Oliveira Cardoso
Data de defesa: 22-02-2018
Programa de Pós-Graduação: Ciências Médicas

BANCA EXAMINADORA DA DEFESA DE DOUTORADO

ALUNO: PAULO AFONSO MEI

ORIENTADOR: PROF. DR. FABIANO REIS

COORIENTADOR: PROF. DR. LI LI MIN

MEMBROS:

1. PROF. DR. FABIANO REIS

2. PROFA. DRA. CLAUDIA DA COSTA LEITE

3. PROF. DR. CELSO DARÍO RAMOS

4. PROFA. DRA. TÂNIA APARECIDA MARCHIORI DE OLIVEIRA CARDOSO

5. PROFA. DRA. DIANA RODRIGUES DE PINA MIRANDA

Programa de Pós-Graduação em Ciências Médicas da Faculdade de Ciências Médicas da Universidade Estadual de Campinas.

A ata de defesa com as respectivas assinaturas dos membros da banca examinadora encontra-se no processo de vida acadêmica do aluno.

Data: 22/02/2018

“Hoje, eu sei quanta serenidade é necessária para que um pai adormeça antes do seu filho”. *José Luís Peixoto*.

Dedico, portanto e necessariamente com o maior peso, às noites em claro enfrentadas por meus pais, Paulo Roberto e Lúcia Helena, na minha juventude, para que eu pudesse ter chegado até aqui. Espero que, daqui para a frente, possam dormir tranquilamente, sabendo que, através de todos os recursos que podiam lançar mão em seus conhecimentos e moral, tenham cumprido a árdua tarefa de educar bem seus filhos.

Queria aproveitar a ocasião para expandir o conceito de “pais”, pois, segundo *Beaumarchais*, “Somos sempre filhos de alguém”. Nesse sentido, e não menos importante, gostaria de agradecer às minhas “segundas mães”, que continuam sendo tão importantes para a minha integridade: Alayde, minha avó materna, e “Dona” Vanilda, que já há tempos ultrapassou a ocupação de minha simples secretária para ocupar o posto de meu braço direito na vida.

AGRADECIMENTOS

Ao meu orientador, Prof. Fabiano Reis, por aceitar o desafio de me ter como seu primeiro orientando em pós-graduação e pela cumplicidade e solidariedade dos bons e maus momentos que ocorrem normalmente nas pesquisas. Que eu possa ser o primeiro de muitos.

Ao Prof. Li Li Min, merecidamente agora cidadão honorário campinense, pelo desafio de me coorientar e por abrir as portas do Laboratório de Neuroimagem para a coleta de dados.

To Prof. Stephen Fraser, for granting me an educational license for SiroSOM. Only one who is not from computer sciences knows how working with GUI softwares rather than having to code eases life.

Ao Prof. Dr. Cleyton C. Carneiro, por me mostrar ser possível e benéfica a interdisciplinaridade entre a Geologia e a Medicina. E ao Cleyton C. Carneiro, sem qualquer título, por ser suporte para os vales e companhia na comemoração dos picos desta montanha-russa que é a vida.

Ao conhecimento técnico de meus amigos, que em algum ponto da pesquisa implodiram significativas pedras no meio de meu caminho, tornando a trajetória muito menos íngreme: Márcio Akyama, Michel Fornaciali, Michelle Kuroda, Rafael Gióra, Rodrigo Soal.

Special Thanks to all of those who at some point assisted me with my English skills: Mrs. Louise Yariv, for being the most dedicated teacher a non-native English speaker could have had in High School, and Mrs. Candice, who kindly did an important review in two of the presented papers.

To the University of Cambridge, on the behalf of Dr. Tomasz Matys, my direct supervisor, and Prof. Fiona Gilbert, head of department, who opened to me the doors to one of the most prestigious universities in the globe.

À CAPES, pelo suporte financeiro através do programa de Doutorado Sanduíche, que se mostrou fundamental para que a pesquisa ganhasse musculatura necessária.

E finalmente para os ilustres desconhecidos que escreveram ou gravaram tutoriais na internet ensinando técnicas de Matlab, Office, etc., ou que construíram programas com GUI para que leigos da computação como eu pudessem completar suas pesquisas.

Por vezes o único meio para realmente encontrar-se é perder-se por completo

Kellie Elmore

RESUMO

Com o advento de conjunto de dados cada vez maiores (Big Data), dentre os quais se incluem imagens médicas com crescente qualidade de resoluções espacial, espectral e radiométrica e, portanto, com maior número de pixels, espectros de varredura e níveis de cinza, faz-se útil o uso de técnicas matemáticas avançadas, especialmente as não-supervisionadas, para aprimorar a segmentação do tecido cerebral em agrupamentos (clusters) distintos, possibilitando uma melhor visualização da área acometida por patologia.

Este trabalho teve por objetivo segmentar imagens de sistema nervoso central (SNC) em patologias de três naturezas distintas – neoplásica (tumores), desmielinizante (esclerose múltipla) e vascular (acidente vascular cerebral isquêmico -AVCi).

Foram realizados três estudos, descritos nos Artigos I, II e III, nos quais foram analisadas imagens de SNC de pacientes (ressonância magnética - RM, nos Artigos I e II, e tomografia computadorizada - TC, no artigo III) com diagnóstico de, respectivamente, neoplasia, esclerose múltipla tipo remitente-recorrente e AVCi. As imagens foram transformadas em matrizes com valores da escala de cinza para cada pixel, em cada aquisição, e processadas por ferramentas com capacidade de execução de Mapas Auto-Organizáveis (SOM), SiroSOM e Weka, que permitiram a construção de mapa neural com treinamento de neurônios e, posteriormente, particionamento dos mesmos em agrupamentos por K-médias. As novas matrizes, com assimilação de clusters para cada pixel, foram novamente reconstruídas em imagens, que foram submetidas à avaliação de médicos com formação consolidada prévia em neurorradiologia.

Os trabalhos I e II confirmam a capacidade geral de segmentação de imagens médicas por meio de SOM com razoável precisão de delimitação de bordas em RM. O artigo III revelou um grau insatisfatório de exatidão de delineação de bordas de lesões à segmentação de TC, porém com potencial identificável de melhora da acurácia se novos e mais amplos estudos forem realizados, com base no material publicado.

ABSTRACT

With the upcoming of ever bigger datasets (Big Data), among those medical images, ever-growing on spatial, spectral and radiometric resolutions and, hence, in the number of pixels, spectrums and digital numbers (DNs), the use of advanced mathematical algorithms, especially non-supervised neural networks, plays a role on improving automated segmentation of the human brain into smaller, distinct clusters, providing a better visualization of the comprised, pathological regions.

This work aimed to segment central nervous system (CNS) images from pathologies of three different natures - neoplasms, demyelinating and vascular (ischemic stroke).

We performed three studies, each one described in distinct articles, I, II and III, on which medical CNS images (MRI for Articles I and II and CT for article III) from patients with confirmed diagnosis of, respectively, neoplasms, relapsing-remitting multiple sclerosis and ischemic stroke were analyzed. The images were transformed in matrices of gray values for each pixel, in each acquisition, and then processed by Kohonen's Self Organizing Maps (SOM) via capable software - SiroSOM or Weka, through training of neurons belonging to the built neural map, followed by clustering by K Means. The newly created matrices with cluster values for each pixel were then rebuilt back to new images that were appreciated by physicians skilled in neuroradiology.

The research confirms the general ability of medical image segmentation by SOM, with reasonable border delimitation in MRI, in articles I and II. Article III revealed a non-satisfactory precision of lesion border delineation on CT, but there is a likely chance of improvement of accuracy, if further, deeper studies based on the publication data could be performed.

LISTA DE ABREVIATURAS E SIGLAS

SIGLA	TERMO em INGLÊS (original ou *sua tradução em itálico*)	TERMO em PORTUGUÊS (original ou *sua tradução em itálico*)
AI	Artificial Intelligence	*Inteligência Artificial*
AVCi	*Ischemic Cerebral Stroke*	Acidente Vascular Cerebral isquêmico
c	Circa (around)	Circa (cerca de)
DBI	Davies-Bouldin Index	*Índice de Davies Bouldin*
EMRR	*Relapsing-Remitting Multiple Sclerosis*	Esclerose Múltipla Remitente-Recorrente
FLAIR	MRI FLuid-Attenuated Inversion Recovery Acquisition	*Sequência de MRI de Aquisição por Recuperação Inversa Atenuada por Fluidos*
Gd	Gadolinium (MRI contrast)	Gadolínio (contraste utilizado em MRI)
h	Height	*Altura*
HC	*General Hospital*	Hospital de Clínicas
ie	id est (that is)	id est (isto é)
LVQ	Learned Vector Quantization	*Quantização de Vetor* Aprendida
NN	Neural Network	*Redes Neurais*
RM	*Magnetic Resonance Imaging (MRI)*	(Imagem de) Ressonância Magnética
SNC	*Central Nervous System (CNS)*	Sistema Nervoso Central
SOM	Self-Organizing (Neural) Maps	*Mapas (Neurais) Auto-Organizáveis*
T1	MRI T1 Sequence	Sequência de MRI T1
T1-Gd	MRI T1 Acquisition with Gadolinium infusion	Sequência de MRI de Aquisição T1 com infusão de Gadolíneo
TC	*Computed Tomography (CT)*	Tomografia Computadorizada
UNICAMP	*University of Campinas*	Universidade Estadual de Campinas
VQ	Vector Quantization	*Quantização de Vetor*
vs	versus	versus
w	Width	*Largura*

SUMÁRIO **Pág.**

SUMÁRIO (cont) **Pág.**

1. INTRODUÇÃO

1.1 PREÂMBULO - Cibernética, Base de Dados, Big Data, Data Mining, Inteligência Artificial, Neurocomputação, Aprendizado De Máquinas, Deep Learning

Há poucas chances hoje de que passemos mais que alguns minutos de nossas vidas sem executar uma tarefa na qual pelo menos algum dos passos não tenha sido auxiliado direta ou indiretamente por um computador. Neste sentido, podemos dizer que vivemos em um mundo governado pela interface humano/máquina, como imaginara Wiener (1), valendo-se em 1948 da expressão grega κυβερνήτης – kibernetes (”governar”), para cunhar o termo *cibernética* como a comunicação real-virtual, à época ainda um conceito demasiadamente abstrato.

Computadores vêm evoluindo em velocidade de processamento e multimodalidade de dados, conforme vamos progressivamente transferindo aos mesmos mais tarefas que eram executadas primariamente por humanos, ou inserimos novas tarefas, antes impossíveis de se realizar. Da mesma forma, à medida em que precisamos executar tarefas cada vez mais complexas, a quantidade de dados que querermos avaliar - *Database* ou Base de Dados - torna-se progressivamente maior.

Numa era em que temos uma quantidade massiva de dados - *Big Data*, faz-se imperioso que saibamos como “peneirar”, ou extrair do conjunto de dados apenas aqueles que nos interessam e organizá-los, de forma que façam sentido para o objetivo proposto. Assim, o objetivo de *Data Mining* (Mineração de Dados), como o nome sugere, é o de encontrar relações, por vezes não óbvias, que permitam a classificação de dados de diferentes maneiras, muitas vezes por agrupamentos (*clusters*), de acordo com o desejo/objetivo do usuário, dando significado aos dados analisados. Desde os anos 60 já havia a ideia de que a separação automática se faria necessária (2), mas somente com o passar dos anos, com volume de dados em Big Data cada vez mais robusto, houve maior exploração referente ao tema.

Um exemplo de Big Data são imagens médicas, como por exemplo de Ressonância Magnética (RM) e Tomografia Computadorizada (TC), uma vez que cada imagem é composta de camadas topográficas, cada uma contendo centenas a milhares de pixels, as menores unidades possíveis – os "átomos" - de uma figura, sendo que, no caso de imagens em escala de cinza, como em RM e TC, esses têm valores individuais de 0 a 255, representando os tons de uma escala de cinza *8-bit* (ie, 2^8 ou 256 tons de cinza). Uma mesma imagem médica fornece informações de de diferentes tipos (3), como: quantidade de pixels, densidade dos pixels, quantidade de bandas/espectros medidos (ex: T1, T2 e FLAIR) e intensidade de níveis de cinza para cada aquisição.

Num sentido lato, podemos dizer que, sempre que usamos o computador para minerar Big Data, estamos nos valendo de processos de Inteligência Artificial – *Artificial Intelligence* (AI). AI não envolve exclusivamente interação com Big Data, mas é parte fundamental do processo. A **Figura 1** ilustra em que universo ou conjunto pode ser enquadrado cada um dos termos principais (descritos sempre em itálico e com sublinha tracejada) usados nesse relatório. A **Figura 2** demonstra, na linha do tempo, a data (às vezes estimada) em que a maioria dos termos técnicos usados na descrição passaram a ser usados em publicações científicas.

Figura 1 - Organograma dos termos usados em computação de dados

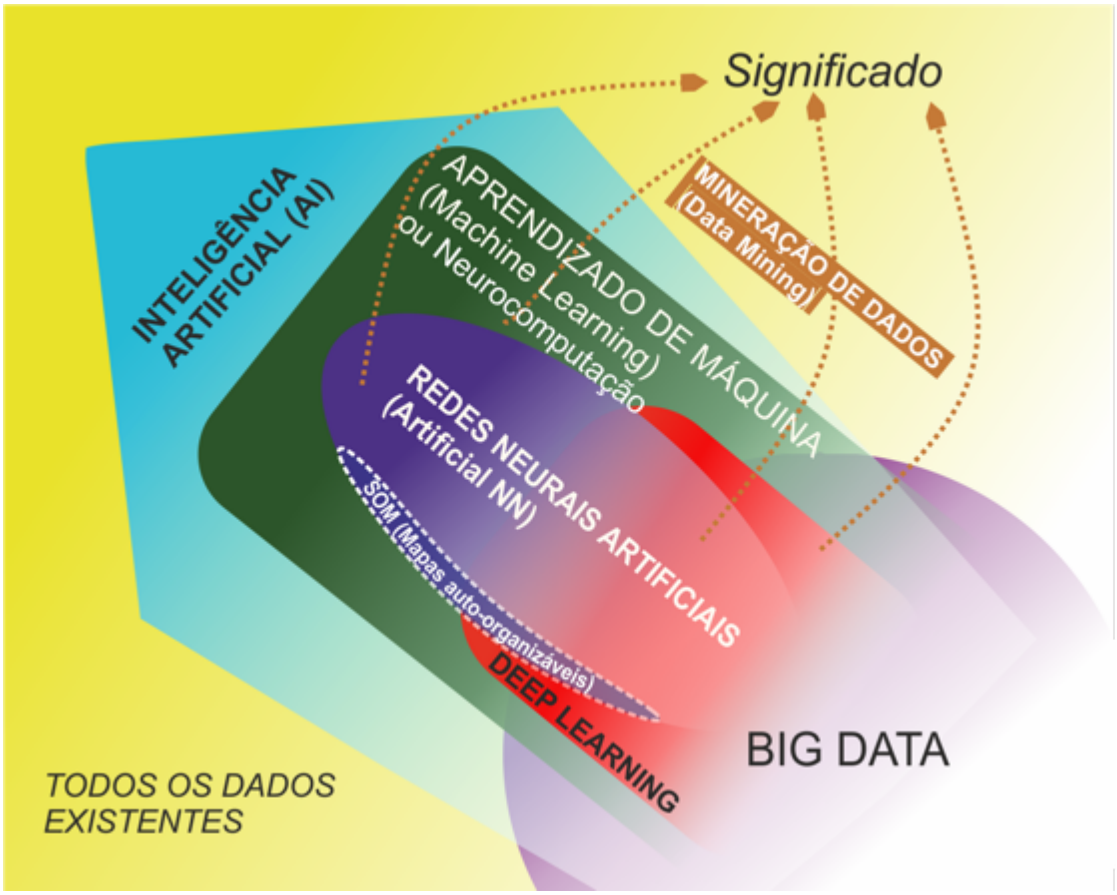

Figura 2 - Linha do tempo para alguns termos relacionados à neurocomputação

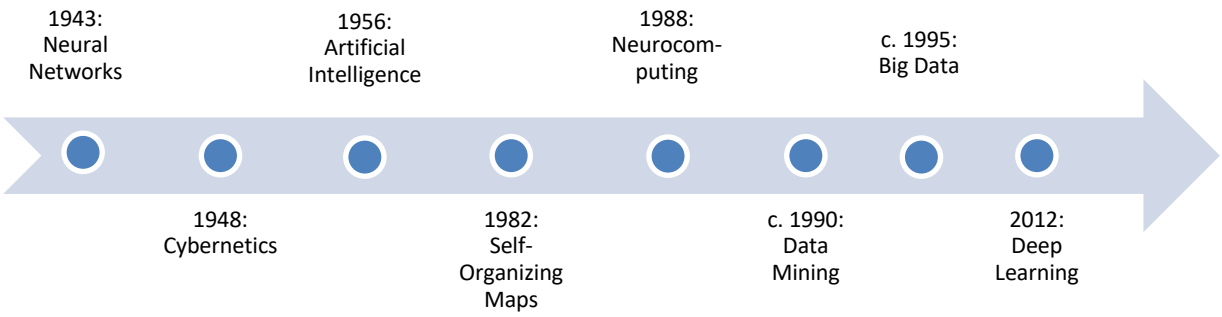

AI, termo cunhado em 1956, em Conferência do Datmout College, New Hamphshire, por McCarthy (4), pode ser compreendida como o ramo da

computação que dispõe de *algoritmos* (sequência de regras e procedimentos) sentenciados a simular o raciocínio humano que, em essência, percebe as informações de seu ambiente e toma decisões/ações que permitam melhorar o sucesso de uma tarefa desempenhada, num esquema simplificado de como um sistema biológico, como por exemplo o cérebro, faria.

Nas últimas duas décadas, contudo, vem crescendo certo desalinho referente à quantidade de tarefas ou técnicas que são englobadas sob a etiqueta de AI, uma vez que, à medida que a computação avança, tarefas mais simples, que não envolvem propriamente o aprendizado de novos conceitos, formas de classificação ou reconhecimento de novos problemas, tendem a não mais serem chamadas de AI, mas simplesmente de *tecnologia de rotina* (ex: o reconhecimento de escrita manual) (5). Uma solução que vem sendo conveniente, no campo da AI, é inserir computadores com real capacidade de aprendizado – *neurocomputadores* - num grupo mais restrito de AI, a chamada *Narrow AI* (AI Restrita) ou *Machine Learning* (Aprendizado de Máquinas). A **Figura 3** apresenta um organograma resumido do exposto acima. Portanto, neurocomputadores são máquinas de aprendizado cuja AI Restrita se processa a partir de algoritmos, normalmente baseados em *Redes Neurais - Neural Networks (NN)*[1]. Os *Mapas Auto-Organizáveis – Self Organizing Maps (SOM),* peças centrais desta tese, constituem um tipo particular de Rede Neural, como veremos nos próximos parágrafos.

[1] Há ainda, mais recentemente, o conceito de *supercomputadores*, que podem trabalhar com massivas quantidades de dados (Big Data) e inserir uma enorme quantidade de camadas no processamento de informações complexas, conceito que vem sendo chamado de *Deep Learning* (Aprendizado Profundo) (5), cujo conceito não será aprofundado no manuscrito, por não fazer parte do escopo da tese

Figura 3 - Limites da abrangência e hierarquização de alguns termos em Neurocomputação, tradução livre do original em inglês. Fonte: (6)

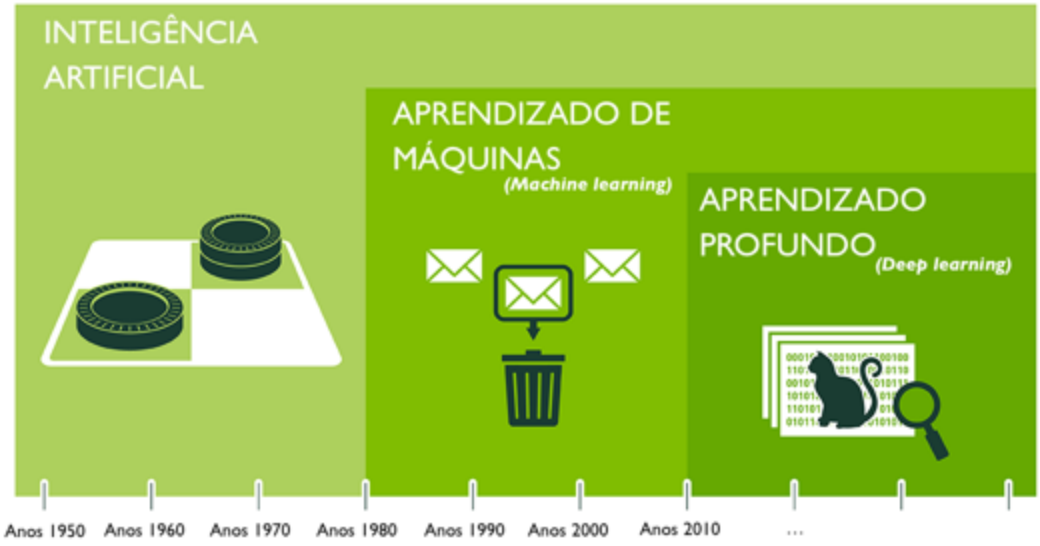

É necessário começarmos, antes de que tenhamos pleno domínio de onde pisamos e para onde damos cada passo na pesquisa com Mapas Auto-Organizáveis – SOM ou Self Organizing Maps, situá-los dentro dos contextos histórico e hierárquico na cibernética, para não nos perdermos enquanto navegamos este grande mapa, que apresenta muitas subderivações e termos distintos para conceitos iguais ou parecidos.

1.2 REDES NEURAIS [ARTIFICIAIS] (NN ou ANN)

1.2.1 Noções Gerais

O Conceito de NN não é uniformemente usado por diversos autores, recebendo uma série de nomenclaturas alternativas e por vezes com significados e contextos que podem muito ou pouco variar, tais como *Neural Computing* (Computação Neural ou Neurocomputação),

Parallel Distributed Processing (Processamento Paralelo Distribuído)[2], *Connection Science*/Connectionism (Ciência da Conexão/Conexionismo).

Uma das características mais marcantes da matemática aplicada é a de, em grande parte das vezes, por inspiração maior da Natureza, tentar traduzir ou replicar o funcionamento de um modelo biológico em um modelo matemático. Nesse sentido, nada mais natural que se inspirar no funcionamento do órgão mais complexo, em termos de redes e conexões, que é o cérebro humano.

Entenda-se, porém, que no atual momento científico é impossível replicar com exatidão as trilhões de comunicações que existem num órgão possuidor de cerca de 100 bilhões de células (7). Assim, há de se ter em consideração, obviamente, que as NN não são a tradução matemática literal do sistema biológico (cérebro), e sim um *modelo*, no sentido computacional, ou seja, uma representação simplificada de algo mais complexo, que enfoca em aspectos-chave do funcionamento do sistema, da mesma forma que não considera aspectos secundários não importantes para a simplificação (8).

A história das NN pode ser plotada numa semi-reta, com início no trabalho revolucionário de McCuloch e Pitts, em 1943 (9), continuando com uma série de publicações subsequentes desde então, aparte um hiato histórico no final da década de 1960 e maior parte da década de 1970, por divergências autorais e relegação do estudo das redes ao ostracismo. Novos trabalhos, desde então, vêm surgindo em um ritmo exponencial e progressivamente mais detalhado e complexo, com alto interesse econômico em pesquisa e desenvolvimento das mesmas.

O primeiro modelo de NN, Perceptron (10), assim como os modelos descritos em seguida, lidavam com dados em única camada, o que provou-

2 - O termo *paralelo* refere-se ao tipo de processamento usado por um neurocomputador. Enquanto um computador convencional processa as informações uma a uma, o que é chamado de *em série*, o neurocomputador processa mais que uma informação de uma vez, ou seja, *em paralelo*, através de uma rede complexa de conexões, normalmente na forma de redes neurais - NN

se limitado para a resolução de problemas mais complexos, sendo que a aplicabilidade prática, em larga escala, de NN, deu-se de fato após a publicação de modelos propondo o uso de multicamadas - em geral com muitas camadas intermediárias ocultas, como o algoritmo de backpropagation, nos anos 80 (11) (12), um dos mais usados até hoje em redes Feed-Forward.

Sejam uni ou multicamadas, NN são um processo em distribuição paralela (13), baseada em máquina de estado finito (Finite State Machine) - um modelo computacional, cujas unidades básicas/elementares são chamadas *nodos* ou *neurônios* (ambos termos equivalentes) (14). Isso implica, basicamente, no fato de que lidamos com um modelo dinâmico de resposta a estímulos, no qual há mudança do *estado* (Q) do sistema conforme variam-se o tempo (t) e os estímulos (S) recebidos, o que implica em diferentes respostas (R), simplificado nas equações a seguir:

$$Q(t+1) = G(Q(t), S(t))$$

$$R(t+1) = F(Q(t), S(t))$$

Estes neurônios têm a capacidade de serem treinados (15). Análogos aos neurônios cerebrais, os neurônios artificiais poderão receber, tal como um neurônio biológico recebe dos dendritos, um ou mais sinais de entrada ("*inputs*", na **fig. 4A** ou "X_n", na **fig. 4B**), e a estes são atribuídos diferentes pesos sinápticos (w_n, na **fig. 4B**). Os inputs são processados, normalmente em múltiplas camadas, no corpo do neurônio – este normalmente com o papel de integrar os diferentes pesos sinápticos (w_n) e então ativá-los (por funções que podem variar geralmente entre threshold, linear ou não-linear), devolvendo-os num único sinal de saída (*output* na **fig. 4A** ou y na **fig. 4B**), que pode ser um sinal de qualquer natureza matemática desejada (16).

Figuras 4A a e 4B– Exemplo Esquemático de Processamento do Neurônio na NN

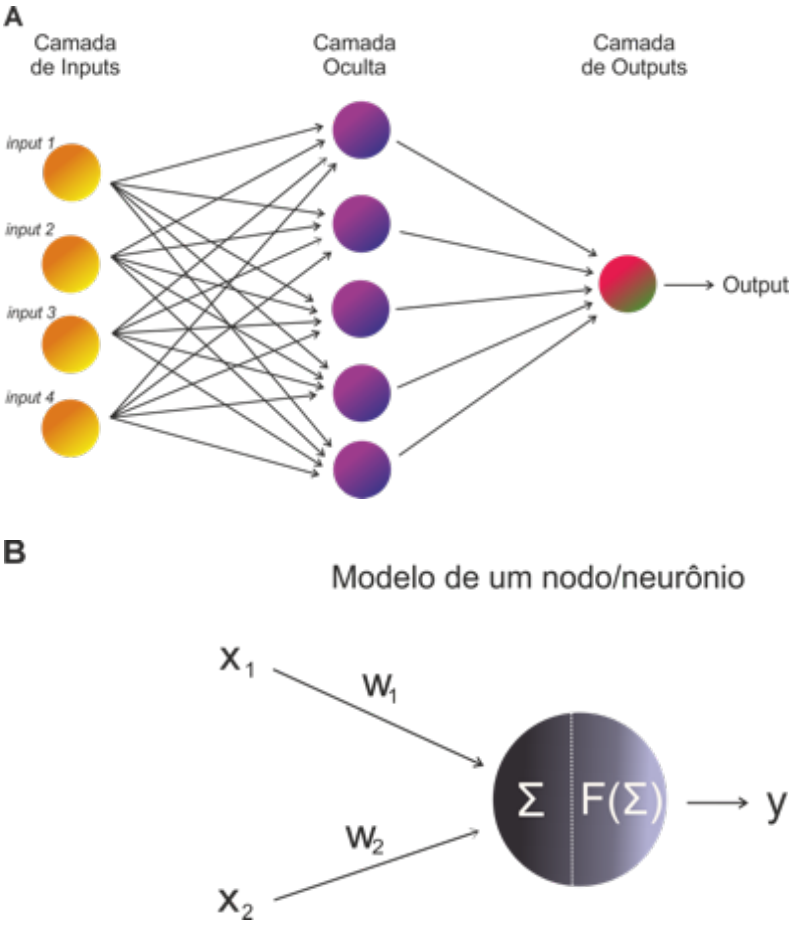

NN são, assim, usadas largamente em dois principais ramos de Data Mining: classificação de dados multi ou n-dimensionais (ambos termos são equivalentes) em padrões ou categorias distintas, bem como fazer predições condicionais à maneira que análises estatísticas o fazem (17).

Com o avanço da tecnologia da informação, as NN têm tido papel cada vez mais de destaque na programação de tarefas cada vez mais complexas e/ou que almejem resultados cada vez mais precisos. O próprio *Deep Learning*, ou, em tradução livre, Aprendizado Profundo, tão em voga na mídia atual, nada mais é que uma evolução da complexidade e do número de camadas ocultas disponíveis no arranjo de uma NN, o que quase invariavelmente demanda capacidade de processamento maior que de computadores convencionais, através dos ditos supercomputadores.

Apenas como modo de situarmo-nos no contexto atual, o infográfico da **Figura 5**, abaixo, é uma representação simplificada (em inglês) das diferentes arquiteturas dos principais tipos de NN disponíveis no momento.

Figura 5 - Infográfico esquemático dos principais tipos de NN existentes atualmente - Fonte: (18)

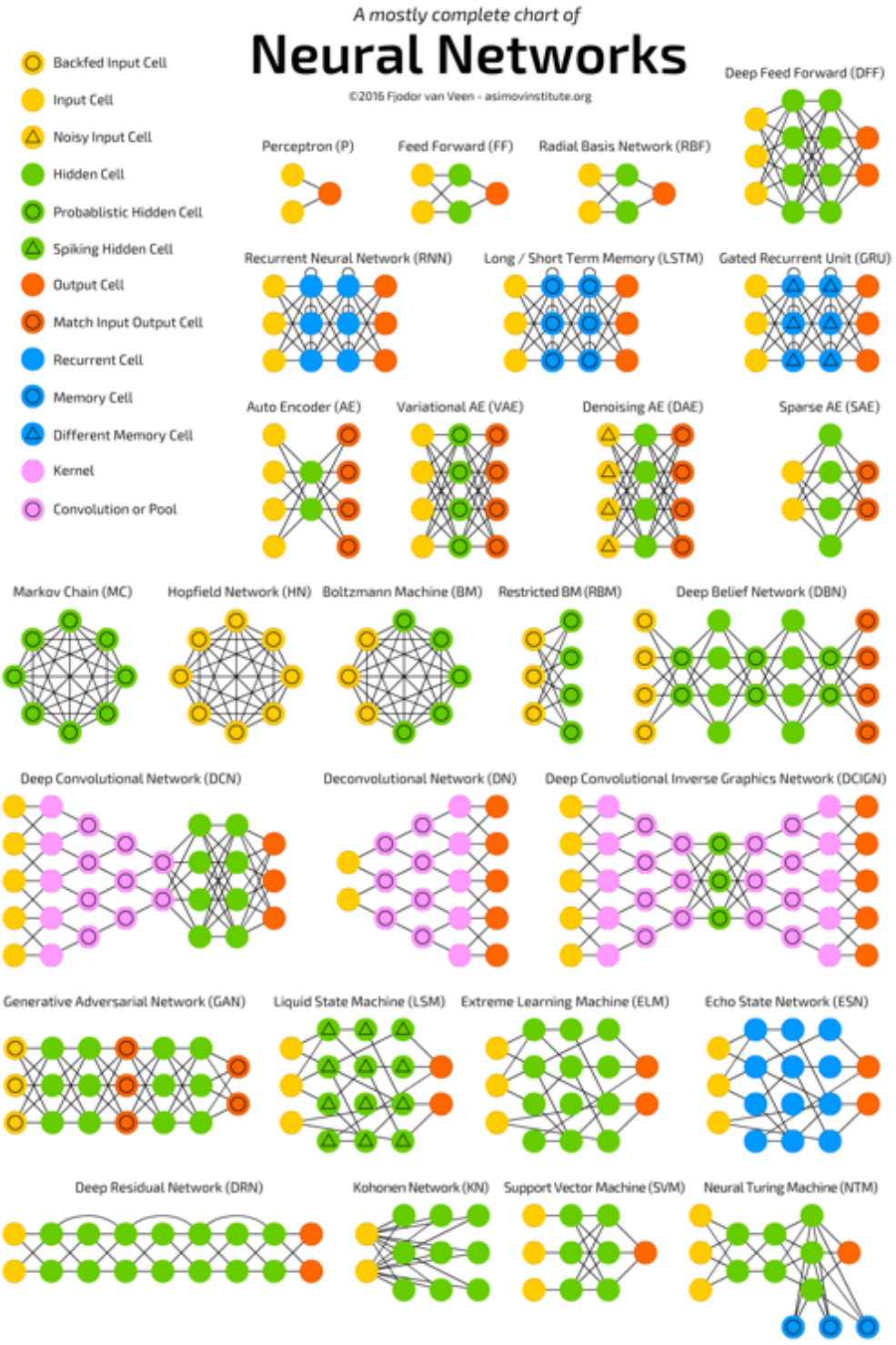

Embora existam múltiplas formas de se classificar NN, para efeitos práticos, cabe a divisão didática, para compreensão deste manuscrito, das NN em dois subgrupos principais, baseados em seus respectivos formatos de aprendizado, descritos a seguir e esquematizados simplificadamente na **Figura 6**:

a) NN SUPERVISIONADAS: redes que treinam, baseadas em exemplos fornecidos previamente, para dar respostas-alvo (target responses) desejadas para novos problemas. Em outras palavras, aprendem por um "professor externo".

b) NN NÃO-SUPERVISIONADAS (também chamadas de NN Auto-Organizáveis[3]): não há resposta-alvo ou qualquer tipo de informação fornecida como correta previamente à análise. Não há "professor externo". Os SOM, processamento usado nos artigos desta tese, encontram-se nessa categoria.

Figura 6- Esquema de Redes Neurais com os subtipos mais corriqueiros. Fonte: (8)

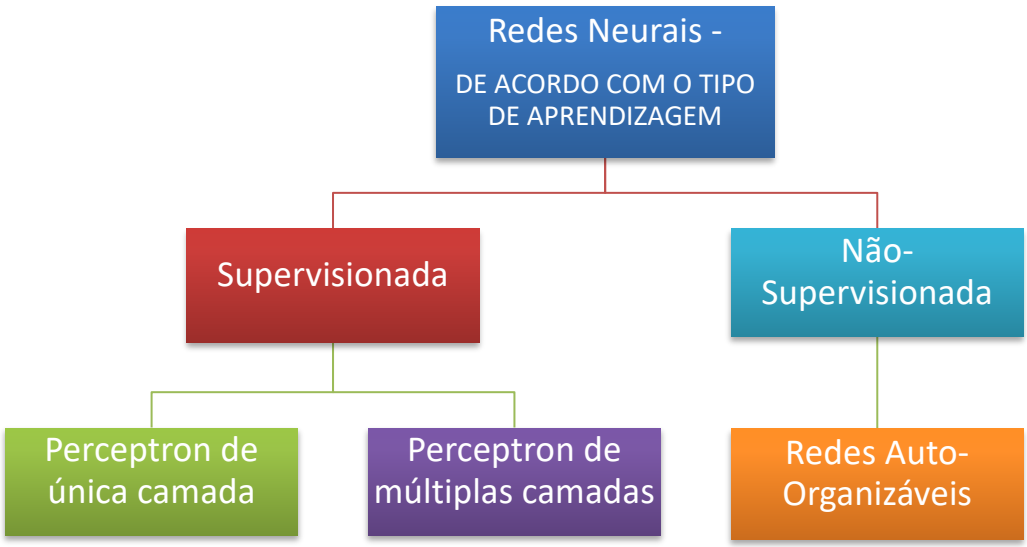

3 - Alguns autores divergem quanto à similaridade entre os termos NN Não-Supervisionadas e NN-Auto-Organizáveis. Neste artigo, optou-se pela equiparação dos termos, conforme Nordbotten (8)

1.2.2 Mapas Auto-Organizáveis – Self Organizing Maps ou Redes de Kohonen

De volta à década de 1950, o assunto dominante nas rodas de estudantes do campo de ciências exatas era certamente o de aprendizado de máquinas e AI. Um dos graduandos que se mostrou interessado pelo tema era o finlandês Teuvo Kohonen, conforme o mesmo explica resumidamente, em um momento biográfico de uma palestra (19). Após a graduação, especializou-se no reconhecimento de padrões – de voz, inicialmente, nos anos 1970, baseando-se em trabalhos sobre Quantização Vetorial (VQ) Clássica, evoluindo para o conceito de SOM, a partir de 1981.

Os SOM, como muitas outras NN, se baseiam na simplificação da informação (redução de dimensionalidade) presente em um conjunto relativamente grande de dados, pela análise não de todo seu conjunto, mas sim de um subconjunto com tamanho menor (geralmente definido pelo usuário) de neurônios representativos daquela população como um todo. Guardadas as proporções, poder-se-ia fazer uma analogia na qual todos os elementos fossem cidadãos e, havendo a impossibilidade de se ouvir todas as queixas individuais, eleger-se-iam "vereadores" que representassem homogeneamente o total da população local.

Em SOM, assim como em outras NN, cada "vereador" é chamado de nodo ou neurônio, conceito previamente explicado no item 1.2.1 (Noções Gerais). Estes são criados em posições aleatórias e neutras, num espaço n-dimensional (mapa) de tamanho configurável, com largura 'w' e altura 'h' sendo, portanto, o número de neurônios $n = w \times h$, onde $n \geq 2$, sendo então posteriormente *treinados*. O treinamento (aprendizagem) divide-se em uma primeira etapa, na qual nodos competem entre si (*aprendizado competitivo*), obedecendo o princípio de *winner-takes-all* - o vencedor, uma espécie de neurônio-chave, chamado de *Best Matching Unit* (BMU) (20), leva tudo - e numa segunda, na qual neurônios vizinhos auxiliam no

reposicionamento adequado do BMU, para que este represente os dados originais da forma mais fidedigna (*aprendizado cooperativo*).

A cada passo a mais em seus treinamentos, os nodos são realocados e seus valores representativos crescem, ou seja, ficam mais próximos de representar com fidedignidade uma subpopulação de dados, à medida que vão se distanciando de representar todos os demais dados. Em outras palavras, o arranjo de neurônios e BMUs no SOM é nada mais que um diagrama de similaridade. Quanto mais próximo fisicamente um neurônio treinado está de outro, mais similares são, enquanto representantes do conjunto maior de dados.

Essas características de proximidade ficam mais explicitadas com a geração de um *mapa auto-organizado* em uma superfície de projeção, sob a qual os neurônios resultantes preservam suas respectivas relações topológicas. Ou seja, em um mapa projetado resultante, neurônios adjacentes permanecem próximos, enquanto que neurônios distantes no espaço n-dimensional preservarão essa distância. Uma das maneiras de representar os mapas ato-organizados resultantes é através da matriz de distância unificada (*Matriz-U*, U-Matrix) (21), na qual os neurônios são classificados em cores que representam a distância entre sua vizinhança no espaço n-dimensional.

Dessa forma, na Matriz-U, convencionalmente cores frias são apresentadas para nodos/neurônios mais próximos ou similares, enquanto que cores quentes são utilizadas para representar neurônios distantes ou dissimilares, conforme exemplo da **Figura 7** (22). Nesta, nota-se um mapa de 99 neurônios (w = 9, h = 11), sendo numerados, no mapa, os BMUs do conjunto. Neste exemplo, e levando-se em conta a distribuição espacial dos nodos e BMUs e de cores, nota-se que os neurônios 1 e 7 são provavelmente bastante similares, ao passo que o neurônio 13 é menos similar a 1, mas ao mesmo tempo é mais similar do que, por exemplo, o neurônio 15 ao neurônio 1.

Figura 7- Exemplo de Matriz U. Fonte: (22)

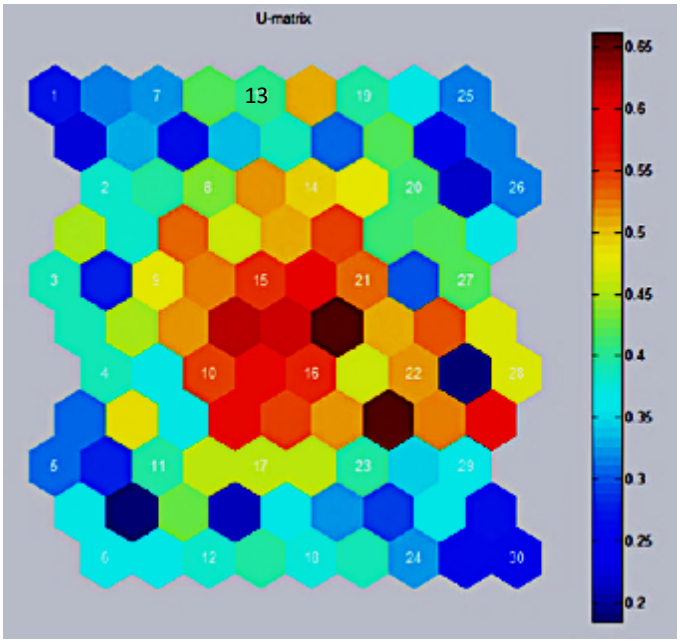

A representação em mapa favorece ao processo de reconhecimento de padrões, uma vez que este processo organiza a informação segundo as características das variáveis analisadas. Desse modo, a informação de entrada se organiza topologicamente, favorecendo os mecanismos do agrupamento que será executado na sequência.

1.2.3 Clustering ou Agrupamento

A separação de dados em grupos por semelhança pode ser chamada, dependendo do autor/artigo, de *clustering* (termo original), ou *agrupamento* de dados.

O agrupamento pode ser feito de forma hierárquica ou não-hierárquica (23) (Gan, Ma, & Wu, 2007), também chamada de particional, opção que interessa à aplicação em neuroimagem, uma vez que não há maior relevância/dominância, na imagem, de um grupo em relação ao outro, independente da relevância clínica que cada agrupamento terá futuramente, na interpretação clínica.

Diversos algoritmos de clusterização são descritos em literatura (24), sendo os mais comuns:

- K-means (K-médias)
- Fuzzy C-means
- Hierárquico
- Gaussiano
- Quality Threshold (QT)
- MST based
- Density based
- Kernel k-means

Em todos os casos desta pesquisa (artigos I, II e III) a segmentação dos neurônios treinados por SOM foi realizada através de K-Médias.

1.3 A Neurogia e Redes Neurais

O uso de técnicas de inteligência artificial não é algo exatamente novo entre pesquisadores no campo da neurologia. Ao contrário, é empregado no auxílio de problemas diversos, como por exemplo encontrar padrões epileptiformes no eletroencefalograma (25) (26) ou segmentar estágios do sono automaticamente na polissonografia (27) (28), ou mesmo responder a questões mais complexas ou abstratas, como predizer o sexo do paciente pela proporção de ritmos diferentes (alfa, beta, gama e delta) no traçado encefalográfico (29). No campo dos distúrbios extrapiramidais, é descrito o uso de NN radiais para prever tremores na Doença de Parkinson, fazendo com que eletrodos de estimulação profunda (Deep Brain Stimulation ou DBS) consumam bateria apenas nos momentos de necessidade e fiquem hibernantes, com baixo uso de energia, nos períodos livres de tremor, prolongando a vida útil da bateria implantada no subcutâneo (30).

O uso de NN na segmentação de neuroimagens vem gradativamente sendo tomado por uso de ténicas mais complexas, em geral redes neurais de

aprendizado profundo (31), ou mesmo tendo maior foco na segmentação em imagens funcionais. Os SOM seguem essa tendência, havendo, à época da composição desse manuscrito, maior número de artigos recentes descrevendo seu uso em Ressonância funcional (32) (33), mas muito poucos dados referentes à sua exploração no campo das imagens anatômicas (RM e TC convencionais).

2. OBJETIVOS

2.1 Gerais e Hipótese

Avaliar a capacidade/desempenho da técnica de SOM em segmentar de maneira automática, não supervisionada, lesões se SNC de naturezas distintas, obtidas por meio imagens bidimensionais (2D) de RM ou TC.

A hipótese inicial foi de que os SOM devem apresentar capacidade razoável de segmentação das lesões, ao menos em RM, uma vez que há maior disponibilidade de dados literários apontando nesta direção. Esperava-se haver algumas limitações decorrentes da própria natureza complexa de segmentação de imagens médicas, porém a expectativa seria de que a técnica teria desempenho semelhante/não inferior de segmentação quando comparada a outras redes neurais não-Deep Learning.

2.2 Específicos de Cada Artigo

- Artigo I - Analysis of neoplastic lesions in magnetic resonance imaging using self-organizing maps

Avaliação do desempenho dos SOM em segmentar lesões neoplásicas intra-axiais e extra-axiais, supratentoriais, usando dados de FLAIR, T1 e T2 em RM de pacientes selecionados no HC UNICAMP.

- Artigo II - Self-Organizing Maps as A Tool for Segmentation of Magnetic Resonance Imaging (MRI) of Relapsing-Remitting Multiple Sclerosis

Avaliação do desempenho dos SOM em segmentar lesões desmielinizantes de aspectos variados (lesões novas e antigas, de tamanhos distintos), usando dados de FLAIR, T1 e e T1-Gd em RM de pacientes selecionados no HC UNICAMP.

- Artigo III - Use of Triple Smart-Smoothing Filters for Enhancing Unsupervised Segmentation of Normal Controls and Ischemic Stroke Images with Self Organizing Maps in Brain CT Images

Avaliação do desempenho dos SOM em segmentar lesões isquêmicas cerebrais, usando apenas dados de TC, de pacientes selecionados no HC UNICAMP e do Addenbrooke's Hospital, da Universidade de Cambridge.

3. METODOLOGIA

3.1 Critérios de Inclusão

Foram incluídos pacientes de idades distintas, de ambos os sexos, que apresentassem as seguintes patologias:

- Artigo I: Neoplasia de SNC, de qualquer linhagem, desde que a lesão fosse supratentorial e com biópsia confirmatória. N = 14 pacientes (1 Astrocitoma, 1 Meningeoma, 6 Glioblastomas Multiformes, 3 Linfomas Primários de SNC, 2 Oligodendrogliomas, 1 Ganglioglioma);

- Artigo II: Esclerose Múltipla tipo Remitente-Recorrente com pelo menos 1 ano de início dos sintomas, com confirmação clínica pelos critérios de McDonald, indepentente de EDSS e do tratamento no momento da aquisição de imagem. N = 10 pacientes, sendo que 5 apresentavam presença de pelo menos 1 lesão com realce por Gadolínio;

- Artigo III: AVCi de tempos diferentes (hiperagudo, agudo/subagudo e crônico), confirmado por critérios clínicos mais exame de imagem (RM ou TC de perfusão). N = 19, sendo 12 com isquemia cerebral e 7 controles;

3.2 Coleta de dados

As imagens foram coletadas de pacientes provenientes de dois centros de saúde: Hospital das Clínicas – UNICAMP (Artigos I, II e III), e Addenbrooke's Hospital – University of Cambridge (apenas para o Artigo III).

Para os artigos I e II foram usadas imagens axiais de RM (Artigo I: FLAIR, T1 e T2; Artigo II: FLAIR, T1 e T1-Gd) e para o artigo III foram usadas imagens axiais de TC sem contraste.

3.3 Aspectos éticos

A coleta de dados dos pacientes do HC UNICAMP se deu somente após aprovação do Comitê de Ética em Pesquisa, parecer 130.280/2012. Os dados obtidos na University of Cambridge foram autorizados pelo chefe do Departamento de Radiologia e fornecidos pelo médico supervisor local do

estágio no exterior. Em nenhum dos casos houve qualquer contato dos pesquisadores com os pacientes durante a pesquisa ou modificações posteriores em suas condutas após análise de dados.

3.4 Fomento

A pesquisa em solo brasileiro foi feita sem financiamento de órgãos fomentadores. O estágio executado no exterior, no primeiro semestre de 2017, no Departamento de Radiologia na University of Cambridge, recebeu auxílio Capes - Bolsa Sanduíche, processo número 88881.132052/2016-01.

3.5 Desenho dos estudos

Em todos os artigos, tratou-se de estudo retrospectivo de obtenção e análise de imagens adquiridas por pacientes que estiveram ou ainda estavam em tratamento nas instituições detentora dos arquivos de imagens.

3.6 Processamento de Imagens

O infográfico da **Figura 8** esquematiza de forma resumida as etapas do processo, que serão detalhadas a seguir.

3.6.1 Número de dimensões das análises

Em todos os casos, foram realizadas análises por SOM em imagens 2D, ie, não houve reconstrução tridimensional das lesões, a partir das fatias topográficas do SNC. Ao invés, foi analisada apenas uma imagem (uma fatia) de cada sequência, que fosse mais representativa qualitativamente da lesão.

3.6.2 Skull stripping e outros pré filtros

Para otimização da análise, as imagens em todos os artigos sofreram remoção digital manual (delineada pelo avaliador caso-a-caso) da calota

craniana e de estrututas adjacentes (skull stripping), preservando-se apenas o tecido nervoso e ventrículos.

Para o Artigo III, houve uso de filtros de suavização inteligente antes da aplicação de SOM, conforme pormenorizado na publicação, anexada.

3.6.3 Conversão de raster para matriz

Em todos os Artigos, foram extraídas das imagens raster (RM ou TC) as matrizes contendo o valor de cinza para cada pixel (para cada aquisição, no caso dos Artigos I e II). O aplicativo usado para essa etapa foi o ArcMap (34), obtido através de licença educacional.

3.6.4 Análise por SOM e Agrupamento

A construção de um mapa de neurônios e seu treinamento, bem como a segmentação posterior por K-Médias, foi executada nos Artigos I e II pela ferramenta SiroSOM, baseada em Matlab, desenvolvido pelo CSIRO, Austrália (35) sob licença acadêmica, e no Artigo III, pelo aplicativo Weka 3, beseado em Java, desenvolvido pela Universidade de Waikato, Nova Zelândia (36). O tamanho do mapa e número de iterações variou conforme o tamanho da matriz, havendo maior detalhamento nos artigos anexados.

Figura 8 - Esquematização das Etapas de Processamento das Imagens

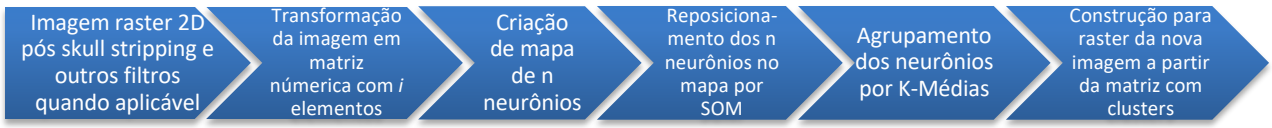

3.6.5 Definição do número de Agrupamentos (Clusters)

A metodologia para a definição do número de agrupamentos *n* ideal para cada imagem variou conforme os artigos. Nos Artigos I e II, optou-se pela definição de acordo com o Índice Davies-Bouldin - DBI, Davies-Bouldin Index

(37), uma métrica de avaliação interna, ou seja, através de cálculos baseados em quantificações e atributos inerentes à base de dados para testar o desempenho de *n* agrupamentos, sendo 1 < n < 25, na qual a solução ótima é representada pela de DBI de menor valor.

Para o Artigo III, foi adotado um valor heurístico de 6 agrupamentos em todos os pacientes e controles analisados.

3.6.6 Conversão da nova matriz para raster

Novamente, através do uso do aplicativo ArcMap, foi feita a transformação da nova matriz gerada em cada análise, contendo os valores de agrupamentos para cada pixel analisado, para nova imagem, e então foram atribuídas cores distintas para cada cluster, para facilitação da visualização.

4. RESULTADOS

4.1 Artigo I (publicado) - Analysis of neoplastic lesions in magnetic resonance imaging using self-organizing maps

Journal of the Neurological Sciences 359 (2015) 78–83

Contents lists available at ScienceDirect

Journal of the Neurological Sciences

journal homepage: www.elsevier.com/locate/jns

Analysis of neoplastic lesions in magnetic resonance imaging using self-organizing maps

Paulo Afonso Mei [a,*], Cleyton de Carvalho Carneiro [b], Stephen J. Fraser [c], Li Li Min [a], Fabiano Reis [a]

[a] University of Campinas (UNICAMP), Brazil
[b] University of Sao Paulo (USP), Brazil
[c] Commonwealth Scientific and Industrial Research Organization (CSIRO), Australia

ARTICLE INFO

Article history:
Received 22 April 2015
Received in revised form 27 September 2015
Accepted 14 October 2015
Available online 23 October 2015

Keywords:
Self-organizing maps
SOM
Magnetic resonance imaging
MRI
Neoplastic
Brain
Tumors

ABSTRACT

Objective: To provide an improved method for the identification and analysis of brain tumors in MRI scans using a semi-automated computational approach, that has the potential to provide a more objective, precise and quantitatively rigorous analysis, compared to human visual analysis.
Background: Self-Organizing Maps (SOM) is an unsupervised, exploratory data analysis tool, which can automatically domain an image into selfsimilar regions or clusters, based on measures of similarity. It can be used to perform image-domain of brain tissue on MR images, without prior knowledge.
Design/Methods: We used SOM to analyze T1, T2 and FLAIR acquisitions from two MRI machines in our service from 14 patients with brain tumors confirmed by biopsies - three lymphomas, six glioblastomas, one meningioma, one ganglioglioma, two oligoastrocytomas and one astrocytoma. The SOM software was used to analyze the data from the three image acquisitions from each patient and generated a self-organized map for each containing 25 clusters.
Results: Damaged tissue was separated from the normal tissue using the SOM technique. Furthermore, in some cases it allowed to separate different areas from within the tumor - like edema/peritumoral infiltration and necrosis. In lesions with less precise boundaries in FLAIR, the estimated damaged tissue area in the resulting map appears bigger.
Conclusions: Our results showed that SOM has the potential to be a powerful MR imaging analysis technique for the assessment of brain tumors.

1. Introduction

Inter- and intraexaminer variability and inconsistency for interpretation of different lesions in the Central Nervous System (CNS), such as tumors, among others (demyelinating, inflammatory, vascular) are routine factors in neuroradiology. Such inconsistencies may lead to wrong diagnoses and inadequate decisions in treatment, which has been discussed by various authors. [2,3].

Tumefactive lesions, either intra or extra-axial, found on brain Magnetic Resonance Imaging (MRI), usually represent a challenge for both the neurologist and the neuroradiologist. Lesion representation on ordinary T1, T2 and FLAIR acquisitions, will depend of histologic nature. For example, intra-axial lesions, glial tumors tend to be hypointense on T1-weighted and hyperintense on T2-weighted, while cerebral lymphomas tend to have isointensity on both T1 and on T2 acquisitions. Isointensity of signal is also the most prevalent aspect on meningiomas, the most common extra-axial lesions. Due to limitations of these routinely-acquired MRI images, and in many cases the lack of diagnostic specificity, the use of complementary advanced methods, such as MRI spectroscopy, perfusion and diffusion weighted MRI are necessary.

A better definition of the margins of a primary lesion would allow better precision for its surgical excision, with less damage to healthy adjacent tissue. Precise extraction being so important for an organ where preservation of millimeters can potentially preserve noble neurological functions. Additionally, better planning of complementary treatment, such as radiation therapy, could be planned. In this context, certain methods of non-visual, automatic classification could assist on the correct nosological classification of diseases.

Self-organizing maps (SOM) is an unsupervised, exploratory data analysis tool, which can automatically domain an image into self-similar regions or clusters, using the principles of vector quantization and measures of vector similarity [8,9]. In a SOM analysis, samples are treated as n-dimensional (nD) vectors in a data space defined by their variables [4]. A reduced number of seed vectors is then typically randomly distributed throughout the nD data space, and these "seeds" are subsequently "trained" via competitive and collaborative processes, over both coarse and fine training cycles (iterations), to represent the structure of the input data. The trained "seed vectors" (now known as best matching units — BMUs) are then projected as nodes onto a

* Corresponding author.
E-mail address: drkult@gmail.com (P.A. Mei).

http://dx.doi.org/10.1016/j.jns.2015.10.032
0022-510X/

Table 1
Profile of the selected patients and SOM processing parameters; RIR = rough (training) initial radius; RFR = rough (training) final radius; FIR = fine (training) initial radius; FFR = fine (training) final radius.

Patient	Age	Sex	Histological diagnosis	Boundaries	Map size	RIR	RFR	FIR	FFR
1	44	M	ASTROCYTOMA	IMPRECISE	68 × 66	95	24	24	1
2	74	F	MENINGIOMA	PRECISE	68 × 66	95	24	24	1
3	44	F	GLIOBLASTOMA	PRECISE	68 × 66	95	24	24	1
4	63	F	LYMPHOMA	PRECISE	68 × 66	95	24	24	1
5	70	F	LYMPHOMA	IMPRECISE	68 × 66	95	24	24	1
6	30	M	GANGLIOGLIOMA	PRECISE	68 × 66	95	24	24	1
7	44	M	OLIGOASTROCYTOMA	IMPRECISE	70 × 68	98	25	25	1
8	30	M	LYMPHOMA	IMPRECISE	58 × 56	81	21	21	1
9	67	M	GLIOBLASTOMA	PRECISE	66 × 64	92	23	23	1
10	58	F	GLIOBLASTOMA	PRECISE	66 × 64	92	23	23	1
11	82	M	GLIOBLASTOMA	PRECISE	66 × 64	92	23	23	1
12	63	M	GLIOBLASTOMA	IMPRECISE	66 × 64	92	23	23	1
13	50	M	OLIGOASTROCYTOMA	IMPRECISE	66 × 64	92	23	23	1
14	62	M	GLIOBLASTOMA	IMPRECISE	66 × 64	92	23	23	1

typically two-dimensional rectilinear map, in such a manner as to maintain, as best possible, their topological relationships in nD space. The resulting "Self Organized Map" is a two dimensional, rectilinear representation of the input multi-dimensional data set. Each node on the "map" may then represent a number of similar input samples; and nodes or groups of adjacent nodes, may represent natural clusters or domains within the original data set.

SOM has gained widespread acceptance for the analysis and integration of disparate data in many diverse fields [24], in a way that provides extra significance to the interpretation. SOM has been used for the interpretation of images in fields such as geology [19] and physics, but also for non-image data analysis in many equally diverse fields, such as the economy and speech recognition. However, its use in medicine overall, in the area of neuroradiology, has been limited.

SOM has been applied to functional magnetic resonance imaging (fMRI) [10,11], but there are few scientific reports on its use for interpretation of conventional MRI images for anatomic interpretation. Li and Chi [2] in 2005, described the successful use of SOM for separating different anatomic portions on MRI of healthy individuals. With respect to diseases specifically, only a limited number of publications were found: one that mentioned the use of SOM for improving the analysis of apparent diffusion coefficient in Alzheimer [5]; another on the spectroscopy of Parkinson patients [6]; and, a third on the analysis of images of head injured patients [7]. Specifically for the analysis of brain neoplasms, Vijayakumar et al. [1] successfully used SOM to separate both high and low grade tumors, edema, necrosis and spinal fluid from healthy tissue.

Several authors have conducted studies based on different segmentation methods. In two recent articles, Bauer et al. (2013) [13] and Menze et al. (2014) [14] conducted reviews testing over 20 tumor segmentation algorithms. However, only very few of those were unsupervised – like the ones performed by Shin [15,16,17], by means of hybrid clustering and image regression, which is a linear generalized method, producing a categorical response. In contrast, SOM, which is not mentioned in any of those reviewed studies, including its use on Vijayakumar's article, has a non-linear method which produces a continuous response based on similarity obtained from vector quantization.

This present study aims to explore and expand the knowledge of SOM's use in medical imaging. Therefore, we will emphasize the clustering of similarity produced by a self-organized map.

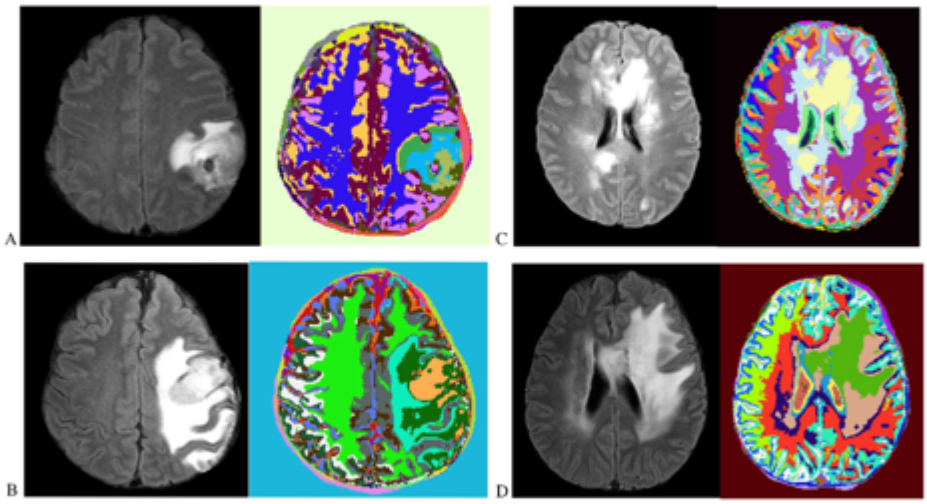

Fig. 1. Examples of lesions from four patients in comparison between FLAIR and the SOM-based image. On A (GBM) and B (GANGLIOGLIOMA), examples of lesions categorized as having PRECISE boundaries, and on C (LYMPHOMA) and D (ASTROCYTOMA), lesions with IMPRECISE boundaries.

Table 2
Values in gray scale obtained from T1, T2 and FLAIR acquisitions, divided into 3 subgroups, according to the median principle.

	T1	T2	FLAIR
Low	0–80	0–51	0–78
Medium	81–109	52–92	79–110
High	110–255	93–255	111–255

2. Materials and methods

We collected T1, T2 and FLAIR, brain MRI acquisitions that represented the same topographic level of the lesion in 14 patients from both sexes, with ages from 30 to 82 years. The patients, who attended our University Hospital, were diagnosed with brain tumors, of different origins - primary glial, neuroglial, meningo-epithelial coating, or lymphomas, all histologically confirmed. The lesions were then, based on FLAIR and SOM interpretation, classified up to their boundaries (lesion + surrounding edema) as PRECISE (when there seemed to be a more clear limit and a better cluster differentiation for sick tissues) or IMPRECISE (when otherwise). Patient data can be found on Table 1. All self-organized maps were built using a toroidal shape and hexagonal lattice, with a Gaussian neighborhood kernel. Training lengths were 20 iterations for the "Rough" training and 400 for the "Fine" training cycles.

All images were obtained twice, using both 1.5 and two 3 Tesla Philips MRI systems, located at our University Hospital. The topography of the images chosen for each patient was the best representation of the lesion. Hence, 3 images for each patient were used for the SOM analysis.

Images were then standardized with regard to their resolution, size and X and Y axis positions on the encephalon. After which, they were plotted using the ArcGis Desktop software, which allowed the conversion to point data containing the X and Y values for each pixel, and their gray scale value (0 to 256). For each patient, a Microsoft Excel table was then created containing all this information.

The data sheet for each patient was processed and analyzed by SiroSOM software, a Matlab-based SOM implementation available from CSIRO (Australia). We generated different sized maps in accordance with the heuristic rule [18], as displayed in Table 1 using random seeding of the data space, and a total of 20 rough, then 400 fine iterations. Our examination of these data sets showed that this combination of iterations produced maps that were interpretable and adequate for our purpose. A toroidal surface was used for projection purposes. After the self-organized map was created, we clustered the SOM node-values using a K-means with 25 clusters, as our examination of these

Table 3
Values of T1, T2 and FLAIR of clusters representing the neoplastic tissue, as well as their correspondence with values of the means obtained in Table 2.

Patient	Acquisition	Mean value of clusters representing pathological tissue (neoplasm)*	Interpretation
1 (Astrocytoma)	T1	65, 96	Low-to-medium T1
	T2	108, 143	High T2
	FLAIR	151, 190	High FLAIR
2 (Meningioma)	T1	37, 47, 65	Low T1
	T2	139, 158, 162	High T2
	FLAIR	166, 195, 196	High FLAIR
3 (Glioblastoma)	T1	27, 44, 94	Low-to-medium T1
	T2	137, 148, 161	High T2
	FLAIR	147, 181, 187	High FLAIR
4 (Lymphoma)	T1	110	High T1
	T2	132	High T2
	FLAIR	119	High FLAIR
5 (Lymphoma)	T1	107, 137	Medium-to-high T1
	T2	102, 143	High T2
	FLAIR	107, 149	Medium-to-high FLAIR
6 (Ganglioglioma)	T1	103, 92, 18	Medium-to-high T1
	T2	73, 66, 70	MediumT2
	FLAIR	48, 43, 39	Low FLAIR
7 (Oligoastrocytoma)	T1	62	LowT1
	T2	124	High T2
	FLAIR	197	High FLAIR
8 (Lymphoma)	T1	134, 150, 160	High T1
	T2	83, 61, 45	Medium T2
	FLAIR	239, 178, 140	High FLAIR
9 (Glioblastoma)	T1	144	High T1
	T2	126	High T2
	FLAIR	147	High FLAIR
10 (Glioblastoma)	T1	48, 63, 83	Low T1
	T2	121, 157, 200	High T2
	FLAIR	151, 185, 196	High FLAIR
11 (Glioblastoma)	T1	42, 76, 94	Low-to-medium T1
	T2	6, 115, 117	High T2
	FLAIR	24, 85, 87	Low-to-medium FLAIR
12 (Glioblastoma)	T1	87, 96, 109	Medium T1
	T2	61, 79, 141	Medium-to-high T2
	FLAIR	77, 102, 202	Medium-to-high FLAIR
13 (Oligoastrocytoma)	T1	82, 88, 91	Medium T1
	T2	87, 114, 157	Medium-to-high T2
	FLAIR	151, 186, 214	High FLAIR
14 (Glioblastoma)	T1	72, 74	Low T1
	T2	25, 41	Low T2
	FLAIR	125, 142	High FLAIR

*The cluster(s) assigned as representative of tumors were the ones that were present in the same region as the tumor in FLAIR and characteristically showing asymmetry between hemispheres, which infers that the tissue is abnormal in comparison to healthy tissues, symmetrical in both hemispheres.

Table 4
Obtained measures, in pixels, with the image selection tool, for FLAIR and SOM.

Patient, diagnosis and boundary type	FLAIR	SOM
1 Lymphoma, imprecise	37,876	39,102
	38,949	38,526
	36,074	37,953
2 Ganglioglioma, precise	76,093	69,295
	79,015	72,197
	75,439	77,751
3 Glioblastoma, precise	31,963	30,776
	32,512	28,754
	31,501	29,523
4 Meningioma, precise	57,604	56,956
	58,171	56,066
	60,172	57,421
5 Lymphoma, imprecise	152,470	169,754
	137,208	169,446
	145,556	164,710
6 Astrocytoma, precise	76,601	95,760
	78,014	97,263
	80,204	96,346
7 Oligoastrocytoma, imprecise	43,645	34,844
	40,859	36,686
	37,155	37,660
8 Lymphoma, imprecise	11,446	11,826
	11,339	11,363
	12,206	10,805
9 Glioblastoma, precise	44,804	37,100
	42,888	39,340
	47,358	36,835
10 Glioblastoma, precise	99,019	104,974
	101,484	106,372
	87,638	105,871
11 Glioblastoma, precise	66,362	66,096
	71,733	65,391
	65,029	61,261
12 Glioblastoma, imprecise	146,729	228,673
	131,885	236,298
	141,415	225,056
13 Oligoastrocytoma, imprecise	159,760	229,467
	167,112	253,028
	156,522	229,541
14 Glioblastoma, imprecise	78,147	106,488
	79,838	105,561
	79,432	107,546

data sets showed that this combination of iterations produced maps that were interpretable and adequate for our purpose.

A new table was then created by the software, correlating each pixel to its respective cluster. The data were transformed into a new shape archive, by Oasis Montaj software. The files were then converted to rasters by ArcGis Desktop, and one final image with clusters separated by distinct colors was mounted for analysis.

Following, for each patient, an estimation of the area of the lesion on the most representative topography was measured, by the same skilled examiner, using FLAIR acquisition - which is, along with T2, the most used for estimation of lesion size, and comparing it with the size on SOM. The image capturing tool was used on both cases, to obtain an estimated size in pixels, and three measures were taken for each acquisition, for each patient, to obtain a mean.

3. Results

Some of the generated images can be seen in Fig. 1, as well as the original FLAIR image in each case.

3.1. Lesion detection

In all cases, the SOM-generated image successfully separated the neoplastic lesion and its surrounding edema in one or more distinctive clusters from the other clusters representing other portions of the encephalon.

3.2. Signatures

The gray scale values, (excluding the null values, which represented pixels outside the boundary of the patients' head) ranging from 1 to 256, for each pixel of each image, were grouped together into a single datasheet, according to their acquisition group (T1, T2 and FLAIR). Using the median principle [12], we subdivided each group into thirds, based on numerical order. The groups were then named Low, Medium and High for each acquisition, as shown on Table 2.

The clusters representing abnormal tissue were analyzed, and based on the mean values of T1, T2 and FLAIR, a profile of each tumor was then traced, as detailed in Table 3.

3.3. Estimated lesion area

For comparative analysis and to assess the information content of the SOM-derived image versus the FLAIR-acquired image, the size of the area representing the lesion was measured in each scenario.

For each set of SOM-derived and FLAIR-acquired images, the same examiner manually delineated the area of the lesion, three separated times per image, using an image analysis pixel counting tool. The same examiner was used to reduce the between-examiner variability, which is known to be greater than an individual's variability for measures [3]. The area of the lesion was calculated in pixels, and the results for each group compared statistically.

The lesion area data from both FLAIR and SOM are represented on Table 4.

Exploratory analysis of data, through standard measures (mean, standard deviation, minimum, median and maximum), was performed. The repeatability of each method and comparison among methods was determined by ANOVA for repeated measures [20,21,22,23], with the variables transformed in ranks. The comparison between the two methods, among precise and imprecise lesions' images was made by

Table 5a
Position and dispersion measures for each one of the measures for both methods.

	N							
Method	Obs	Repetitions	N	Mean	S.D.	Minimum	Median	Maximum
FLAIR	14	Rep1	14	77,322.79	46,729.67	11,446.00	71,227.50	159,760.0
		Rep2	14	76,500.50	44,684.50	11,339.00	74,873.50	167,112.0
		Rep3	14	75,407.21	44,811.87	12,206.00	70,234.00	156,522.0
SOM	14	Rep1	14	91,507.93	71,080.25	11,826.00	67,695.50	229,467.0
		Rep2	14	94,020.79	75,801.77	11,363.00	68,794.00	253,028.0
		Rep3	14	91,305.64	70,225.52	10,805.00	69,506.00	229,541.0

p-Value for ANOVA to repeated measures with the response variable transformed in ranks.
Method: 0.8538.
Repetition: 0.2672.
Repetition*method: 0.6185.

Table 5b
Comparison SOM vs FLAIR for measures of A — all lesions, B — precise lesions, and C — imprecise lesions. Comparison p-value was obtained through Wilcoxon.

	A SOM (all) vs FLAIR (all)	B SOM (precise) vs FLAIR (precise)	C SOM (imprecise) vs FLAIR (imprecise)
Z	−1,161[a,b]	−1,183[c]	−2,028[b]
Asymp. Sig. (2-tailed)	,245	,237	,043

[a] Wilcoxon Signed Ranks Test.
[b] Based on negative ranks.
[c] Based on positive ranks.

the Wilcoxon test. Non-parametric tests were adopted due to the limited samples. The significance level adopted was of 5%.

ANOVA results are shown in Table 5a. No significant differences were found between the repetitions, meaning that each method presented repeatability. Also, there were no differences between measure methods, which means they measured images in a similar fashion.

With respect to the difference between lesion areas in FLAIR and SOM, there was no significant statistical difference when all measures were compared ($p = 0.245$, Table 5b), nor when PRECISE boundaries lesions were compared ($p = 0.237$, Table 5b). However, when only imprecise lesions were compared, the difference on the measure of the areas in FLAIR and SOM did significantly differ ($p = 0.043$, Table 5b). Wilcoxon test was used for this comparison [20,21,22,23].

4. Discussion

Despite having a limited number of samples, and being aware of some limitations of representativeness that it would imply, we were able to successfully analyze, through SOM, tumors of different natures (glial, neuroglial, meningothelial, lymphomas), with the correct separation of each into different clusters, based on normal versus pathological tissue.

Besides the correct separation of different areas of the lesions, as already shown previously to be possible by Vijayakumar [1] and again replicated in this current work, we explored the subject of a tumor's signature and the lesion size manually estimated on SOM-derived enhancements versus conventional acquisitions, which had not previously been scientifically researched.

Our tumor signatures' evaluation showed that different tumors do behave differently in T1, T2 and FLAIR, depending on their nature, which is in accordance with the previous literature. However, we emphasize the fact that all lymphomas presented medium-to-high intensity values in all three acquisitions, as well as 5 out of 6 Glioblastomas had high intensity values for FLAIR.

With respect to our evaluation of an examiner's ability to delineate a lesion's area, we note that the presumably neoplasmic tissue, in some cases (especially in lesions with imprecise boundaries), appears to be larger when using visual analysis on the conventional acquisition in MRI (T1, T2 and FLAIR) compared to a similar analysis on SOM-derived images. This overestimation may be related either to vasogenic edema (observed, for instance, in meningiomas that compromise venous draining), or can represent tumoral infiltration of the adjacent brain tissue. However, to prove this, new studies would be necessary, including one with microscopic analysis of fragments removed by stereotaxy.

5. Conclusions

SOM is an under exploited tool for the analysis of medical images. The results of this study show that a SOM analysis may assist in the separation of tumors from healthy tissue as distinct clusters on MRI acquisitions.

The SOM clusters attributed to unhealthy tissue presented distinct T1, T2 and FLAIR signatures, depending on the nature of the neoplastic lesion. Furthermore, the lesion size estimated by SOM tends to be bigger than that observed by the naked eye for lesions with imprecise boundaries, suggesting that the circumjacent tissue may have alterations not detectable by conventional sequences. However, due to the absence of histopathological correlation and to the small number of cases, the aim of this work was only to initiate a discussion about the use of the SOM vector quantization based technique for the analysis of MRI in neuroradiology, and in potential further research with broader samples and with more advanced techniques, such as the use of biopsy and/or necropsy, is mandatory.

References

[1] C. Vijayakumar, R. GharpureDamayanti, C. Pant, M. Sreedhar, Segmentation and grading of brain tumors on apparent diffusion coefficient images using self-organizing maps, Comput. Med. Imaging Graph. 31 (2007) 473–484.
[2] Y. Li, Z. Chi, MR brain image segmentation based on self-organizing map network, Int. J. Inf. Technol. Vol. 11 (No. 8) (2005).
[3] M. Filippi, M.A. Horsfield, S. Bressi, et al., Intra- and inter-observer variability of brain MRI lesion volume measurements in multiple sclerosis. A comparison of techniques, Brain 118 (1995) 1593–1600.
[4] S.J. Fraser, B.L. Dickson, A new method for data integration and integrated data interpretation: self-organising maps, in: B. Milkereit (Ed.), Proceedings of Exploration 07: Fifth Decennial International Conference on Mineral Exploration 2007, pp. 907–910.
[5] W.P. Dos Santos, R.E. de Souza, P.B. dos Santos Filho, Evaluation of Alzheimer's disease by analysis of MR images using multilayer perceptrons and Kohonen SOM classifiers as an alternative to the ADC maps, Proceedings of the 29th Annual International Conference of the IEEE. EMBS cité internationale, Lyon, France, August 23-26, 2007.
[6] D. Axelson, I.J. Bakken, I. Susann Gribbestad, B. Ehrnholm, G. Nilsen, J. Aasly, Applications of neural network analyses to in vivo 1 H magnetic resonance spectroscopy of Parkinson disease patients, J. Magn. Reson. Imaging 16 (1) (2002 Jul) 13–20.
[7] E.R. Kischell, N. Kehtarnavaz, G.R. Hillman, H. Levin, M. Lilly, T.A. Kent, Classification of brain compartments and head injury lesions by neural networks applied to MRI, Neuroradiology 37 (7) (1995 Oct) 535–541.
[8] T. Kohonen, Self-organizing maps, 3rd extended edition, Springer Series in Information Sciences, Vol. 30, Springer, Berlin, Heidelberg, N. Y., 1995, 1997, 2001
[9] D.L. Davies, D.W. Bouldin, A cluster separation measure, IEEE Trans. Pattern Anal. Mach. Intell. (1979) 224–227, PAMI-1.
[10] L. Hausfeld, G. Valente, E. Formisano, Multiclass fMRI data decoding and visualization using supervised self-organizing maps, NeuroImage 96 (2014 Aug 1) 54–66, http://dx.doi.org/10.1016/j.neuroimage.2014.02.006 Epub 2014 Feb 12.
[11] S.B. Katwal, J.C. Gore, R. Marois, B.P. Rogers, Unsupervised spatiotemporal analysis of fMRI data using graph-based visualizations of self-organizing maps, IEEE Trans. Biomed. Eng. 60 (9) (2013 Sep) 2472–2483, http://dx.doi.org/10.1109/TBME.2013.2258344 Epub 2013 Apr 16.
[12] A.P. Fournel, E. Reynaud, M.J. Brammer, A. Simmons, C.E. Ginestet, Group analysis of self-organizing maps based on functional MRI using restricted Frechet means, NeuroImage 76 (2013 Aug 1) 373–385, http://dx.doi.org/10.1016/j.neuroimage.2013.02.043 Epub 2013 Mar 25.
[13] S. Bauer, R. Wiest, L.P. Nolte, M. Reye, A survey of MRI-based medical image analysis for brain tumor studies, Phys. Med. Biol. 58 (2013) R97–R129.
[14] Menze B, Jakab A, Bauer S, Kalpathy-Cramer J, Farahani K, et al. The multimodal brain tumor image segmentation benchmark (BRATS). IEEE Trans. Med. Imaging, Institute of Electrical and Electronics Engineers (IEEE), 2014, pp.33.
[15] H.C. Shin, M. Orton, D.J. Collins, S. Doran, M.O. Leach, Autoencoder in time-series analysis for unsupervised tissues characterisation in a large unlabelled medical image dataset, Machine Learning and Applications and Workshops (ICMLA), 20th International Conference on, vol. 1 2011, pp. 259–264.
[16] H.C. Shin, Hybrid clustering and logistic regression for multi-modal brain tumor segmentation, Proc. of Workshops and Challenges in Medical Image Computing and Computer-Assisted Intervention (MICCAI' 12), 2012.
[17] H.C. Shin, M.R. Orton, J.D. Collins, S.J. Doran, M.O. Leach, Achinsautoencoders for unsupervised feature learning and multiple organ detection in a pilot study using 4D patient data, IEEE T. Pami 35 (2013) 1930–1943.
[18] J. Vesanto, J. Himberg, E. Alhoniemi, J. Parhankangas, SOM Toolbox for Matlab 5: Technical Report A57, Helsinki, Finland, Neural Networks Research Centre, Helsinki University of Technology, 2000.
[19] Carneiro CC, Fraser SJ, Crósta AP, Silva AM, Barros CEM. Semiautomated geologic mapping using self-organizing maps and airborne geophysics in the Brazilian Amazon. Geophysics, Vol. 77, NO. 4 (July–August 2012); P. K17–K24;

[20] W.J. Conover, R.L. Iman, Rank transformations as a bridge between parametric and nonparametric statistics, Am. Stat. 35 (3) (Aug., 1981) 124–129.
[21] G.A. Milliken, D.E. Johnson, Analysis of messy data, Designed Experiments, Volume I, Van Nostrand Reinhold Company, New York, 1984.
[22] D.C. Montgomery, Design and Analysis of Experiments, 3rd ed. John Wiley & Sons, New York, 1991.
[23] B.G. Tabachnick, L.S. Fidell, Using Multivariate Statistics, 4th ed. Allyn and Bacon, Boston, 2001 966.
[24] M.H. Zuchini, Aplicações de Mapas Auto-Organizáveis em Mineração de Dados e Recuperação de InformaçãoMasters Dissertation Supervising Professor: Fernando José Von Zuben, 2003 University of Campinas – Brazil.

4.2 Artigo II (publicado) - Self-Organizing Maps as a Tool for Segmentation of Magnetic Resonance Imaging (MRI) of Relapsing-Remitting Multiple Sclerosis

Self-Organizing Maps as a Tool for Segmentation of Magnetic Resonance Imaging (MRI) of Relapsing-Remitting Multiple Sclerosis

Paulo Afonso Mei[1], Cleyton de Carvalho Carneiro[2], Michelle Chaves Kuroda[3], Stephen J. Fraser[4], Li Li Min[1], Fabiano Reis[1]

1 - Faculty of Medicine, University of Campinas, Brazil
2- Faculty of Engineering, University of Sao Paulo, Brazil
3 – Faculty of Geology, University of Campinas, Brazil
4 - CSIRO, Australia

Address for corresponding author: drkult@gmail.com

***Abstract* - Multiple Sclerosis (MS) is the most prevalent demyelinating disease of the Central Nervous System, being the Relapsing-Remitting (RRMS) its most common subtype. We explored here the viability of use of Self Organizing Maps (SOM) to perform automatic segmentation of MS lesions apart from CNS normal tissue. SOM were able, in most cases, to successfully segment MRIs of patients with RRMS, with the correct separation of normal versus pathological tissue especially in supratentorial acquisitions, although it could not differentiate older from newer lesions.**

Index Terms* - *Self Organizing Maps, SOM, Magnetic Resonance Imaging, Demyelination, Multiple Sclerosis

I. Introduction

Being one of the most concerning illnesses at present, constant and fast changing on its protocols and medications available, demyelinating diseases, such as multiple sclerosis (MS), are among the leading causes of medical help being sought both in the inpatient and outpatient environment, either due to acute situations, such as the need ofemergency care in case of a relapse of recent onset, as well as prompt neurological consultation for outpatients who experience troubles originating both from the disease and from the side effects medications offer.

MS can be subdivided [13], in accordance to the disease course, between Relapsing-Remitting, Secondary Progressive and Primary Progressive, the first being most prevalent. The use of tools to assure better quality of imaging, in this scenario, is highly desirable and should always be improved.

Currently, Magnetic Resonance Imaging (MRI) plays a key role not only for diagnosis, but also for the evaluation of rate of disease progression. Lesion load on MRI is correlated with disability outcome in MS. In both cases, the examiner needs to gather information from distinct acquisitions, that must be seen separately, one at a time, then ponder which will be the next steps taken, including maintenance or modification of the pharmacological treatment.

In this paper, the use of SOM Self-Organizing Maps (SOM), a neural network multivariate pattern recognition technique is proposed. The computational analysis can aid on the identification of neurological lesions, making diagnosis more robust and therapeutic decisions more precise, providing a better characterization of the geometry and extension of the injury, hence facilitating the identification of compromised regions.

According to Kohonen [4], the biggest advantages of SOM are being a non-supervised technique of segmentation, and being widely used in many fields, such as geology [11, 15], mathematics [16], finances [17] and engineering [18]. Besides, the better performance of SOM among other unsupervised techniques, as principal component analysis (PCA) and independent component analysis (ICA), was demonstrated by Coléou et al. [22], which motivated the choice of this tool.

In medicine, its use is still to become more frequent. SOM has already been validated for segmentation of human tissue in previous works [9, 10]. In neuroradiology, it is more frequently used with functional images (fMRI) [6,7,8], but not so much with conventional images for anatomic interpretation.

Mei et al [1], as Vijayakumar et al [2], have shown that SOM can be successfully used to separate neoplasm from normal tissue in the brain, as well, it can segment different areas of the lesion.

978-1-5090-6638-4/17/$31.00 ©2017 IEEE

MS automatic segmentation could play an important role, as one could be more assured of following the rate of increase of the lesion burden for the same patient, in a more precise way [12]. Abdullah et al, on an article in 2011[3], have shown a supervised training method of segmentation that could predict possible lesions of MS in MRI. However, to our knowledge, no indexed paper so far has further explored the segmentation of MS lesions based on an unsupervised learning technique, as with SOM, among others.

This present study aims to investigate the capability of the assisted segmentation of MS lesions by SOM, as well as to contribute to data on the yet-not-frequent use of SOM in medical research.

II. Materials and Methods

We collected FLAIR, T1 and T1 with Gadolinium (Gd) – with enhancement present in half of the cases – which in this context represents lesions of newer nature brain 1,5 Tesla MRI acquisitions that represented, for the same patient, the same topographic level of the lesion in 10 patients with confirmed diagnosis of Relapsing-Remitting MS, 2 males and 8 females, with ages from 21 to 69 years, as described in Table I. The topography chosen for each patient represented the area with the highest lesion burden. Half had Gd enhancement at the time of the acquisition. MS patients characteristically have lesions of different times of onset, and the enhancement by Gd demonstrates that new lesions have appeared roughly within the last 3 months, and are useful information regarding treatment decision. All patients were under immunomodulating regimen and being regularly followed at our institution on the moment the MRIs used in this research was performed.

TABLE I
Patients Enrolled

PATIENT	AGE	SEX	Gd ENHANCEMENT	LOCATION OF SLICE STUDIED
1	46	M	-	Supratentorial
2	33	F	-	Supratentorial
3	33	F	+	Supratentorial
4	39	F	-	Supratentorial
5	25	M	+	Supratentorial
6	39	F	+	Supratentorial
7	46	F	-	Supratentorial
8	21	F	+	Infratentorial
9	44	F	+	Supratentorial
10	69	F	-	Infratentorial

Gd = Gadolinium

The acquisitions, for each patient, were then pre-processed and registered, in a fashion that their boundaries were mostly coincident. The images were then transformed from raster into points by ArcMap software [21], data was gathered and the absolute black (regions of the pictures that had no brain tissue, with gray scale value of 0 in all acquisitions) suppressed, in a worksheet, with values of gray of T1, T1 Gd and FLAIR for each pixel. Subsequently, the generated matrix ran through SOM, first for training neurons, and then segmenting the neurons in clusters by k-means, using for both tasks SiroSOM, a Matlab-based SOM implementation available from CSIRO, Australia, idealized by Fraser and Dikson [5]. The parameters used for training neurons are displayed in Table II.

SOM is a neural network tool formed by two layers: the input data samples, and the map of nodes, called neurons, that can learn, in a simplified model of brain processing by a iterative method. Let be $x = [x_1, x_2, x_3, \ldots, x_n]$ the sample of n dimensions to be classified, and N the number of samples. The two map dimensions of SOM are heuristic determined by two close numbers whose multiplication is closest to $5 * \sqrt{N}$, and whose ratio is equal to the ratio of the two biggest eigenvalues of the covariance matrix of input data. Each node is associated to a weight (w), with n dimensions, randomly distributed. The target of the algorithm is to adjust the values of weights to better classify the input samples, in this case by Euclidian distance parameter. The vector between the closest node and the sample is called Best Matching Unit (BMU) and is used to update the weighs as follows:

$$w_i(t+1) = w_i(t) + \alpha(t) \cdot h^i_{BMU}(T) \cdot [x_k - w_i(t)] \quad (1)$$

in which t is the iteration, h^i_{BMU} is the radius of neuron neighborhood with hexagonal lattice, which was defined as a Gaussian equation, and determines the neurons to be updated, and α is the learn radius, defined as:

$$\alpha(t) = \alpha_0 / \left(1 + 100\frac{t}{T}\right) \quad (2)$$

in which T is the training length. In this study, the training was done in two parts: an initial one with rough values, and a refined one, with lower values, all shown in table II.

The distance map between the nodes, called U-Matrix, enables the visualization of the clustering results. Once the technique preserves topography, it is possible to visualize closer groups of nodes (in cold colors) representing similar patterns, while more distant ones are associated with disparate patterns.

In order to evaluate SOM performance, two errors are calculated: topographic (Te) that computes the occurrences in which the samples is associated to a BMU that is not adjacent in map structure, and quantization (Qe) that measures how close the input data is to the BMUs.

Because the number of map nodes are big, they are usually clustered by k-means method, in which k is defined by the David-Bouldin index.

III. Results

The most important variables and results of SOM are summarized in table II.

TABLE II
PARAMETERS USED IN NEURON TRAINING BY SIROSOM

Patient	Map Size	Rough Training			Fine Training			Final Qe	Final Te
		Initial Radius	Final Radius	Training Length	Initial Radius	Final Radius	Training Length		
1	64 × 62	90	23	20	23	1	400	0.0114	0,257
2	52 × 50	73	19	20	19	1	400	0,0825	0,083
3	70 × 68	98	25	20	25	1	400	0.0228	0.025
4	68 × 66	95	24	20	24	1	400	0.0048	0.126
5	66 × 64	92	23	20	23	1	400	0.0056	0.153
6	66 × 64	92	23	20	23	1	400	0.0261	0.026
7	68 × 66	95	24	20	24	1	400	0.0171	0.027
8	44 × 42	61	16	20	16	1	400	0.0717	0.087
9	68 ×66	95	24	20	24	1	400	0.0055	0.122
10	44 × 42	61	16	20	16	1	400	0.0232	0.319

On Fig. 1a one can see an example of component plots and the U-Matrix generated in patient 2. The number of clusters c to be created, being $c \in \mathbb{N} \mid 2 \leq c \leq 25$, was defined based on the internal clustering of the Davies Bouldin Index (DBI), provided in SiroSOM, where the lowest value for each analysis indicated the possible best result. Fig. 1b shows an example of plot of the values of DBI for each possible value of c. SiroSOM results were than transformed back from points to raster, including cluster number for each pixel. This transformation allowed the composition, by ArcMap, of one single image, segmented on basis of similarity as explained above.

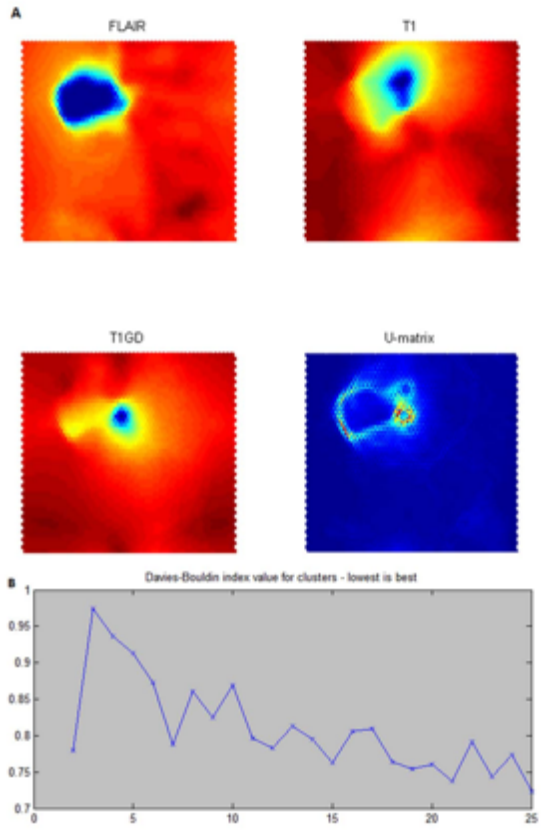

Fig 1 – A. Maps of Components, plotted separately; B. Davies-Bouldin Index values for c clusters, being $c \in \mathbb{N} \mid 2 \leq c \leq 25$

Images obtained by SOM can be seen in Figure 2, alongside with FLAIR and T1-Gd acquisitions of each patient. Each SOM generated image is segmented in colors which represents different clusters.

In all supratentorial images, we are able to notice a complete separation of the lesions in one or two specific clusters, usually with the most hyperintense part of the lesion being put in one cluster, and the lesser bright in another, but both different from the adjacent healthy/healthier tissue. However, for the same patient, lesions with and without Gd enhancement were classified as the same cluster.

In some patients (more prominent on patients 5 and 6), a part of the cortex/juxtacortical area is classified as the same cluster as the lesions.

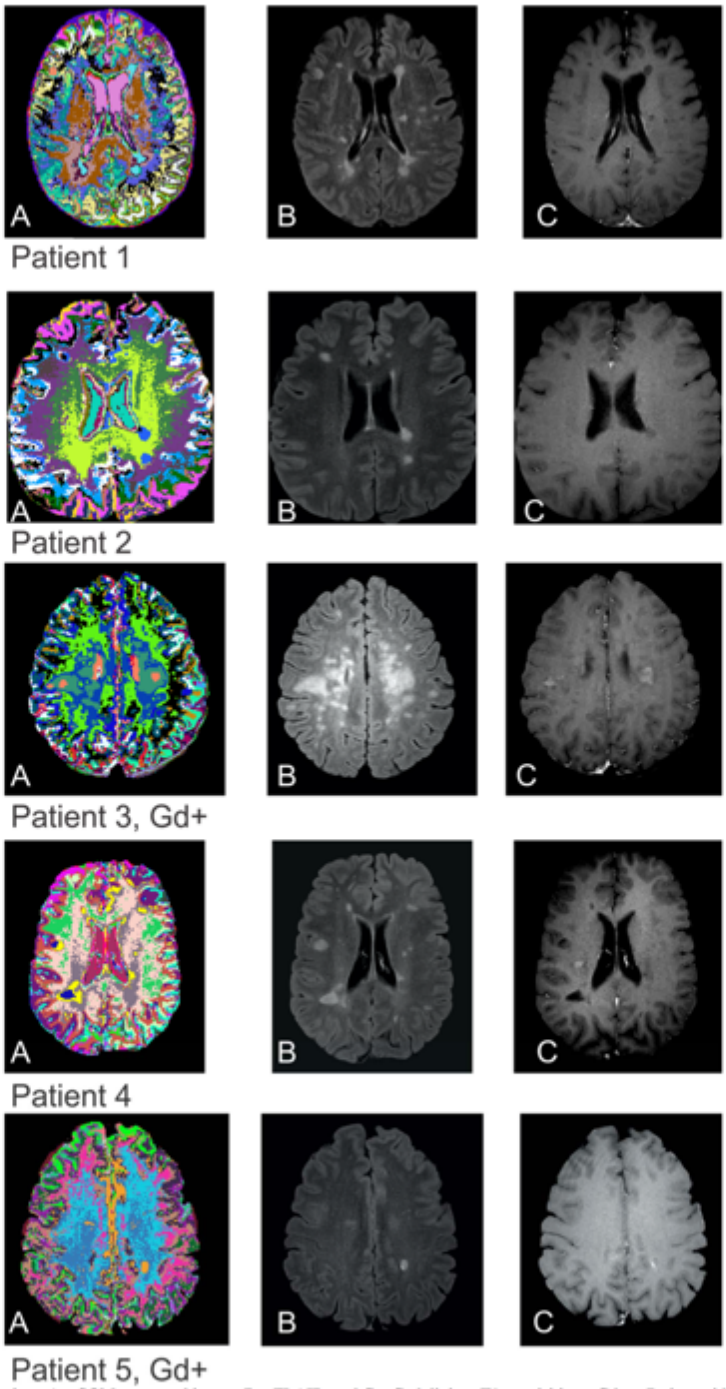

Fig. 2 – For each patient, A – SOM generated image, B – FLAIR, and C – Gadolinium T1 acquisitions. Gd+ = Patient with Gd enhancement.

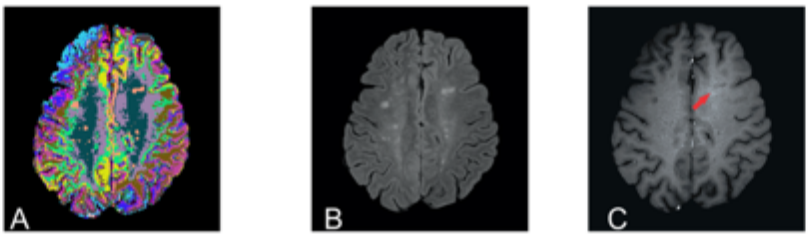

Patient 6, Gd+ (red arrow)

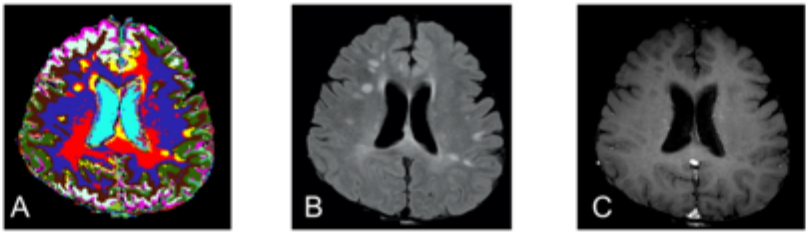

Patient 7

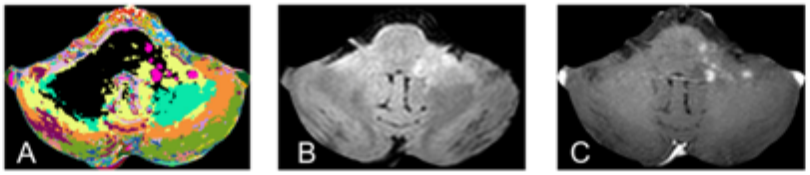

Patient 8, Gd+

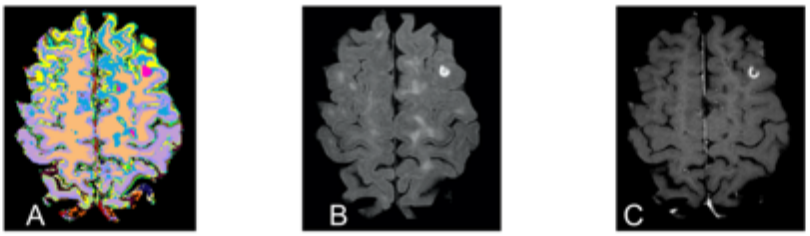

Patient 9, Gd+

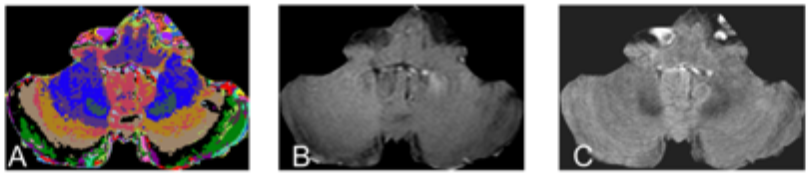

Patient 10

Fig. 2 (contd.) – For each patient, A – SOM generated image, B – FLAIR, and C – Gadolinium T1 acquisitions. Gd+ = Patient with Gd enhancement. On Patient 6 the area of enhancement (shown by red arrow) is better seen in other acquisitions, not displayed here

IV. Discussion

Keeping in mind that we analysed a limited number of samples and that it may carry some limitations of representation, SOM were able to successfully segment MRIs of patients with RRMS, with the correct separation of normal versus pathological tissue in general, and further research would be useful to expand the knowledge on this issue.

As mentioned above, in some patients, cortical and juxtacortical areas are classified in the same cluster as demyelinating lesions. This makes sense, as cortical areas are less myelinated, just like the lesions. However, it is not possible, only by SOM analysis, to exclude disease damage in these parts. It may be plausible, as it has now been known for some time, that MS is not only a white matter disease, and that there may be some inflammation occurring as well in a percentage of these areas cluster-similar to lesions. This is in accordance with the already proven concept of Normal-Appearing White Matter (NAWM) [19,20].

This results come in accordance with some of the previous results of SOM in brain neoplastic lesions, where SOM was able to separate lesions from healthy tissues, as well as cluster suspected areas of infiltration. These areas of suspicion (possible infiltration in neoplasms and possible inflammation/gliosis in MS) could be better accessed in upcoming research, focusing on methods of confirmation, such as biopsy/necropsy.

Though the use of Self Organizing Maps appears to be less effective on the segmentation of infratentorial lesions and also not sensitive enough to separate acute Gd enhanced lesions from lesions of older nature, it was very successful on dealing with supratentorial acquisitions.

V. Conclusions

SOM may be a useful tool for the segmentation of supratentorial lesions and for the quantification of lesion burden, being important in defining lesion load. Its use in medical imaging is yet underexploited, and novel research on neuroimaging should be encouraged, based on positive results obtained so far in the few studies already published and the fact that it is an unsupervised method, making it a diagnostic aid valid for not only people with good background of neuroimaging, but also for people of lesser knowledge (medical students and non-physician health practitioners, for example).

Our analysis suggests that demyelinated regions in MS show better lesion delineation when exploited with the aid of segmenting software, if compared to conventional acquisitions alone, such as T1 or FLAIR.

The fine definition of the geometry of the lesions is not always possible based only on individual analysis of MRI images. The use of the dimensional space defined by the analysed variables by SOM made possible not only the categorical separation of tissues, including damaged ones, but also contributed to the geometrical identification of their scope. Even though this segmentation is not binary (i.e., does not separate normal from abnormal, but rather different classes of tissues, including arranging distinct normal tissues in different clusters), it helps to distinguish lesions, grouped in one single cluster (regardless of lesion age), from other areas of the brain that do not show a clear evidence of disease activity on MRI. This learning is fundamental to the diagnosis, as well as to a more precise identification of affected regions, which may guide clinical decisions in MS.

References

[1] P.A. Mei, C.C. Carneiro, S.J. Fraser, L. Li Min, F. Reis, Analysis of neoplastic lesions in magnetic resonance imaging using self-organizing maps. Journal of The Neurological Sciences, 359:78-83, 2015 doi: 10.1016/j.jns.2015.10.032.

[2] C. Vijayakumar, R. Gharpure Damayanti, C. Pant, M. Sreedhar, Segmentation and grading of brain tumors on apparent diffusion coefficient images using self-organizing maps. Computerized Medical Imaging and Graphics 31 473-484, 2007.

[3] B.A. Abdullah, A.A. Younis, P.M. Pattany, E. Saraf-Lavi, Textural Based SVM for MS Lesion Segmentation in FLAIR MRIs. Open Journal of Medical Imaging, 2011, 1, 26-42 doi:10.4236/ojmi.2011.1, 2005.

[4] T. Kohonen, Self-Organizing Maps. 3rd Extended Edition. Springer Series in Information Sciences, Vol. 30, Springer, Berlin, Heidelberg, New York, 2001.

[5] S.J. Fraser, B.L. Dickson, A New Method for Data Integration and Integrated Data Interpretation: Self-Organising Maps. "Proceedings of Exploration 07: Fifth Decennial International Conference on Mineral Exploration" edited by B. Milkereit, p. 907-910, 2007.

[6] L. Hausfeld, G. Valente, E. Formisano, Multiclass fMRI data decoding and visualization using supervised self-organizing maps. Neuroimage. Aug 1; 96:54-66, 2014. doi: 10.1016/j.neuroimage.2014.02.006.

[7] S.B. Katwal, J.C. Gore, R. Marois, B.P. Rogers, Unsupervised spatiotemporal analysis of fMRI data using graph-based visualizations of self-organizing maps. IEEE Trans Biomed Eng. 2013 Sep;60(9):2472-83. doi: 10.1109/TBME.2013.2258344.

[8] A.P. Fournel, E. Reynaud, M.J. Brammer, A. Simmons, C.E. Ginestet, Group analysis of self-organizing maps based on functional MRI using restricted Frechet means. Neuroimage. 2013 Aug 1; 76:373-85. doi: 10.1016/j.neuroimage.2013.02.043.

[9] Y. Li, Z. Chi, MR Brain Image Segmentation Based on Self-Organizing Map Network. International Journal of Information Technology, Vol. 11, No. 8, 2005.

[10] H.C. Shin, M. Orton, J. Collins, S. Doran, M.O. Leach, "Autoencoder in time-series analysis for unsupervised tissues characterization in a large unlabeled medical image dataset," in Machine Learning and Applications and Workshops (ICMLA), 20th International Conference on, vol. 1. IEEE, 2011, pp. 259–264.

[11] C.C. Carneiro, S.J. Fraser, A.P. Crósta, A.M. Silva, C.E.M. Barros, Semi-automated geologic mapping using self-organizing maps and airborne geophysics in the Brazilian Amazon. Geophysics, Vol. 77, NO. 4, July-August 2012; pp. K17–K24.

[12] E. Geremia, et al, Spatial Decision Forests for MS Lesion Segmentation in Multi-Channel MR Images, Medical Image Computing and Computer-Assisted Intervention, Vol. 6361, 2010, pp. 111-118.

[13] Lublin et al, Defining the clinical course of multiple sclerosis; the 2013 revisions. Neurology 2014; 83:278-286.

[14] M.C. Kuroda, Técnicas de Aprendizagem de Máquina Bio-Inspiradas Aplicadas ao Estudo de Rochas Reservatório [Learning Techniques of Bio-Inspired Machines Applied to the Study of Reservatory Rocks]. Dissertation, University of Campinas, Brazil, 2015.

[15] M.C. Kuroda, A.C. Vidal, A.M.A. Carvalho, Interpretation of seismic multiattributes using a neural network. Journal of Applied Geophysics, Volume 85, October 2012, Pages 15–24.

[16] W.J. Conover, R.L. Iman, Rank Transformations as a Bridge Between Parametric and Nonparametric Statistics. The American Statistician, Vol. 35, No. 3, Aug., 1981, pp. 124-129.

[17] G. Deboek, T. Kohonen, Visual Explorations in Finances with Self Organizing Maps. 1st Edition, Springer, 1998.

[18] T. Kohonen, E. Oja, O. Simula, A. Visa, J. Kanga, Engineering applications of the self-organizing map. Proceedings of the IEEE (Volume:84, Issue: 10, 1996.

[19] T. Zeis, U. Graumann, R. Reynolds, N. Schaeren-Wiemers, Normal-appearing white matter in multiple sclerosis is in a subtle balance between inflammation and neuroprotection. Brain, 2008 Jan;131(Pt 1):288-303 DOI: 10.1093/brain/awm291;

[20] U. Graumann, R. Reynolds, A.J. Steck, N. Schaeren-Wiemers, Molecular changes in normal appearing white matter in multiple sclerosis are characteristic of neuroprotective mechanisms against hypoxic insult. Brain Pathol., 2003 Oct;13(4):554-73.

[21] ESRI 2011. ArcGIS Desktop: Release 10. Redlands, CA: Environmental Systems Research Institute.

[22] Coléou T., Poupon M., Azbel K. Unsupervised seismic facies classification: A review and comparison of techniques and implementation, The Leading Edge, v.22, n.10, 2003, p. 942-953.

4.3 Artigo III (submetido) - Use of Triple Smart-Smoothing Filters for Enhancing Unsupervised Segmentation of Normal Controls and Ischemic Stroke Images with Self Organizing Maps in Brain CT Images

NeuroImage: Clinical
Elsevier Editorial System(tm) for Manuscript Draft

Manuscript Number: NICL-17-1088
Title: Use of Triple Smart-Smoothing Filters for Enhancing Unsupervised Segmentation of Normal and Ischemic Stroke Images with Self Organizing Maps in Brain CT Images

Article Type: Regular Article Section/Category: General Corresponding Author: Mr. Paulo Afonso Mei, MD Corresponding Author's Institution: UNICAMP First Author: Paulo Afonso Mei, MD

Order of Authors: Paulo Afonso Mei, MD; Cleyton C Carneiro, PhD; Li L Min, MD, PhD; Leticia Rittner, PhD; Fabiano Reis, MD, PhD; Tomasz Matys, MD, PhD, FRCR

Abstract: Objective: to investigate the potential of automated clustering of ischemic stroke 2 dimensional (2D) CT images by Self Organizing Maps and if pre-processing of the images by smart-smoothing filters could generate more accurate clustering.

Methods: we selected 10 patients that had had an ischemic stroke (later confirmed by either MRI or perfusion-CT) where non-contrast CT was executed within the hyperacute (up to 4.5 hours) or acute (4.5 to 72h) phase after the onset of the clinical symptoms, and 9 controls (normal MRI or perfusion-CT). We selected a 2D slice of either the ganglionic or immediate supraganglionic level of the brain, in the same fashion that ASPECTS is scored. The images were then preprocessed by three different, smart-smoothing filters on ImageJ, a java-based app, and then transformed into numerical matrices that were analyzed and segmented by the SOM algorithm on Weka 3, a Java based app. The

resulting, post-processed images were rated by 5 individuals, either neurologists or radiologists, blinded to the clinical and demographic information, to see if they considered the left and right halves of each image symmetrical or asymmetrical and also compared by a quantitative value, the Structural Similarity Index (SSIM). Statistical analysis of the results was then performed.

Results: the majority of the raters considered eight out of the 10 stroke cases to have an asymmetrical SOM-generated image, as well as six out of the 9 controls to have a symmetrical image, which resulted in a Sensitivity of 80%, Positive Predictive Value (PPV) of 73%, Specificity of 64%, Negative Predictive Value (NPV) of 75% and Accuracy of 74%. The SSIM values obtained from stroke patients vs normal controls did not differ significantly ($p = 0.213$, Wilcoxon signed-rank test).

Conclusion: our work suggests that a combination of different smoothing filters before SOM analysis performs better than single filtering on avoiding grainy, heterogeneous clusters, and delivering smooth segments with continuous borders. We found acceptable sensitivity, PPV and NPV, suggesting that, even though SOM processing did not show an objective SSIM discrepancy between stroke and normal CTs, qualitative analysis

helped a correct diagnosis in the majority of the cases. This method could be furthermore explored and tested in more subjects, especially the ones in the medical field that need more help with diagnosing ischemic lesions on CTs performed early after ictus, like medical students, nurses and other health professionals.

Use of Triple Smart-Smoothing Filters for Enhancing Unsupervised Segmentation of Normal and Ischemic Stroke Images with Self Organizing Maps in Brain CT Images

Paulo Afonso Mei[1], Cleyton de Carvalho Carneiro[2], Leticia Rittner[1], Tomasz Matys[3], Fabiano Reis[1]

1 – Universidade Estadual de Campinas (University of Campinas), Brazil

2 – Universidade de São Paulo (University of São Paulo), Brazil

3 – University of Cambridge, UK

ABSTRACT

Objective: to investigate the potential of automated clustering of ischemic stroke 2 dimensional (2D) CT images by Self Organizing Maps and if pre-processing of the images by smart-smoothing filters could generate more accurate clustering.

Methods: we selected 10 patients that had had an ischemic stroke (later confirmed by either MRI or perfusion-CT) where non-contrast CT was executed within the hyperacute (up to 4.5 hours) or acute (4.5 to 72h) phase after the onset of the clinical symptoms, and 9 controls (normal MRI or perfusion-CT). We selected a 2D slice of either the ganglionic or immediate supraganglionic level of the brain, in the same fashion that ASPECTS is scored. The images were then preprocessed by three different, smart-smoothing filters on ImageJ, a java based app, and then transformed into numerical matrices that were analyzed and segmented by the SOM algorithm on Weka 3, a Java based app. The resulting, post-processed images were rated by 5 individuals, either neurologists or radiologists, blinded to the clinical and demographic information, to see if they considered the left and right halves of each image symmetrical or asymmetrical and also compared by a quantitative value, the Structural Similarity Index (SSIM). Statistical analysis of the results was then performed.

Results: the majority of the raters considered eight out of the 10 stroke cases to have an asymmetrical SOM-generated image, as well as six out of the 9 controls to have a symmetrical image, which resulted in a Sensitivity of 80%, Positive Predictive Value (PPV) of 73%, Specificity of 64%, Negative Predictive Value (NPV) of 75% and Accuracy of 74%. The SSIM values obtained from stroke patients vs normal controls did not differ significantly ($p = 0.213$, Wilcoxon signed-rank test).

Conclusion: our work suggests that a combination of different smoothing filters before SOM analysis performs better than single filtering on avoiding grainy, heterogeneous clusters, and delivering smooth segments with continuous borders. We found acceptable sensitivity, PPV and NPV, suggesting that, even though SOM processing did not show an objective SSIM discrepancy between stroke and normal CTs, qualitative analysis helped a correct diagnosis in the majority of the cases. This method could be furthermore explored and tested in more subjects, especially the ones in the medical field that need more help with diagnosing ischemic lesions on CTs performed early after ictus, like medical students, nurses and other health professionals.

Introduction

Automated segmentation of Computed Tomography (CT) images has been always challenging. In contrast with Magnetic Resonance Imaging (MRI), where one tends to find smooth-border, cohesive clusters, the use of algorithms for unsupervised segmentation in CT without any pre-processing usually fails to provide a satisfactory outcome, with grainy clusters not forming closed, homogeneous polygons/shapes within the image. Therefore, filtering is a mandatory process to obtain better results from clustering (1).

Smoothing filters can usually reduce the graininess common in CT images, however usually at the cost of reducing the sharpness of edges and corners, which could negatively impact the precision of determining the cluster's perimeter. Therefore, the use of structure-preserving smoothing filters is not only desirable, but can also lessen the mitigation of correct border recognition of simple smoothing. There is a number of open source algorithms for "smart smoothing" available for use, among them Smallest Univalue Segment Assimilating Nucleus (SUSAN) (2), Conditional Mean or Bilateral filter (3), and Anisotropic Diffusion (4).

Self-Organizing Maps (SOM) are a computational method developed in 1982 by Teuvo Kohonen (5) and relies on a technique of neuron-vector training that can be used for a variety of tasks, such as missing data prediction and clustering. It has been used successfully for the segmentation of brain MRI of healthy patients (6) and patients with brain lesions, such as neoplasms (7) (8) and Multiple Sclerosis (9). However, to our best knowledge, its use in CTs for brain ischemic lesions has not yet been documented.

We propose in this article a method for segmentation of CT brain images relying on a combination of three different smoothing pre-filters combined with unsupervised clustering with SOM. We demonstrate the practical use of this method by analyzing CT images from patients with acute ischemic stroke. We chose to analyze ischemic as imaging findings in acute infarct are subtle and diagnosis can be challenging even for trained specialists such as radiologists and neurologists, posing an even bigger challenge for other medical staff, such as general practitioners and medical students.

Materials and Methods

We collected 2D axial CT images of either the ganglionic or immediate supraganglionic levels (corresponding to the images used in ASPECTS (10) method of scoring of anterior circulation infarcts) from 10 patients who had a recent ischemic stroke and had CT performed within possible thrombolysis time - i.e., up to 4.5 hours (11) of onset (hyperacute), or from 4.5 to 72 h (acute), confirmed by a complementary method (CT perfusion, repeat CT or MRI), and 9 patients without an infarct who underwent scanning for different reasons. Patients from both groups did not statistically differed in neither age ($p = 0.086$) or male/female ratio ($p = 0.655$) (both calculated by Wilcoxon signed-rank test). Patient 2 had had a previous infarct prior to the current event. The list of patients is shown in Table 1.

PATIENT NUMBER	AGE	SEX	DIAGNOSIS
1	53	M	Acute Left Middle Cerebral Artery (MCA) infarct
2	21	F	Ancient right MCA stroke plus acute left MCA infarct
3	70	M	Hyperacute Right Posterior Cerebral Artery (PCA) infarct
4	69	F	Acute Left MCA infarct with hemorrhagic transformation
5	76	F	Acute Left MCA infarct
6	33	F	No Stroke
7	69	M	No Stroke
8	66	M	Hyperacute Right PCA Infarct
9	84	M	Hyperacute Right MCA Infarct
10	65	F	Hyperacute Left MCA Infarct
11	78	F	Hyperacute Left MCA Infarct
12	70	M	No Stroke
13	65	M	Acute Right MCA infarct
14	70	F	No Stroke
15	54	M	No Stroke
16	35	F	No Stroke
17	45	M	No Stroke
18	12	M	No Stroke
19	60	M	No Stroke

Table 1 – Assigned patients

The skull was stripped manually in Adobe Photoshop and the resulting brain images were processed using Fiji build (12) of ImageJ (13), an open source, Java-based medical image processing and analysis software. The files were first transformed into 8-bit images, whenever it was not already the case. Subsequently, the outliers were removed (radius = 10 pixels, threshold = 50), and contrast equalization was performed twice using Contrast Limited Adaptive Histogram Equalization (CLAHE) (14) filter (blocksize = 127, histogram bins = 256, maximum slope = 1.50). At the end of this stage, the image was converted to a matrix of gray intensity values by ArcMap, an integral part of ArcGIS bundle (15), and then segmented in an unsupervised fashion, by SOM, using Weka 3 (16), a Java based tool for data mining. A heuristic value of 6 clusters was chosen for the output matrix. Attributes for SOM segmentation were: height = 3, width = 2, learning rate = 1.0, convergence Epochs = 1.000, ordering epochs = 2.000. Conversion to matrix and segmentation were repeated each time an additional smoothing filter was applied (SUSAN filtering, additional Anisotropic Diffusion and additional bilateral

filter). The filtering steps are exemplified in fig. 1. The matrices of six clusters each were then transformed back to images, with a color code being assigned randomly (not according to intensity ranges) for each cluster (either gray, orange, light blue, dark blue, green or red). Colors of high contrast were chosen for better visualization.

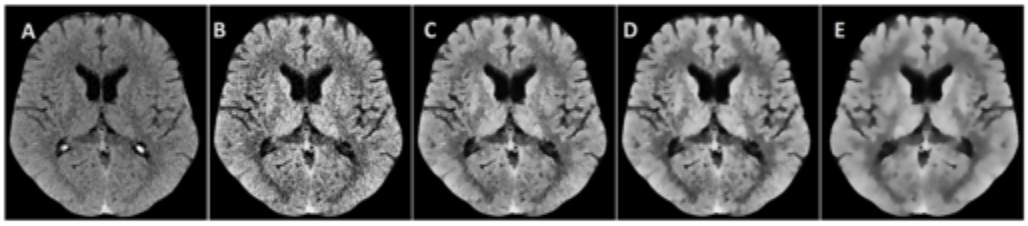

Fig. 1 – every step of image filtering for patient 6, from the original acquisition to the final result:
A = original
B = image A after removal of outliers and CLAHE filter (Fiji) applied twice
C = image B after SUSAN filtering (Fiji)
D = Image C after Anisotropic Diffusion Filter (Fiji)
E = Image D after Bilateral Filter (Fiji)

The resulting images were assessed by five independent professionals (neurologists or radiologists) blinded to the clinical and demographic information (such as presence of infarct, age or sex). The raters were asked to evaluate the images for symmetry between the right and the left hemispheres judging similar color assignment for the same topographical areas/structures between contralateral hemispheres. Each examiner independently classified the images as being “mostly symmetrical” or “mostly asymmetrical”. Then, a patient was considered definitely asymmetrical only if at least three raters agreed, otherwise it was considered symmetrical.

Lastly, for a quantitative analysis, each resulting image was divided in two halves, each half containing half of the encephalon and of the same height and width, hence containing the same amount of pixels. These two halves were compared using a similarity score, the Structural Similarity Index (SSIM) (17). The SSIM values can be seen in Table 2a.

Results

Examples of each step of filtering and clustering can be seen in figs. 2a and 2b. Figure 3 shows the original CT, the final cluster color assignment and a FLAIR MRI of the infarct of patients 3, 4 and 5. In all patients, background was successfully separated from the encephalon since the first round of clustering, being the ventricles in most cases included in the same clustering as the one used for the background, indicating an already expected proximity of the intensity values of cerebrospinal fluid to zero (absolute black, the value of the background pixels), whereas in the remaining cases, another cluster (represented in orange in patients 1 and 2, in fig. 2a, and in patient 4, in fig. 3) occupied the majority of the ventricles and the outermost border of the hemispheres, as well as, in patient 2, the majority of the territory of an old infarct, indicating low values of intensity in these areas.

In the majority of cases the telencephalon could be distinguished from the basal ganglia and the diencephalon. Also, the clusters assigned for the deep white matter of the hemispheres differed from the one(s) assigned to the cortex and subcortical white matter.

The classification of images by the examiners as being either Symmetrical or Asymmetrical can be seen in Table 2a. Eight out of 10 cases with infarct were considered Asymmetrical, while six out of nine controls were considered Symmetrical, demonstrating Sensitivity of 80%, Positive Predictive Value (PPV) of 73%, Specificity of 64%, Negative Predictive Value (NPV) of 75% and Accuracy of 74%. The SSIM values obtained from stroke patients vs normal controls did not differ significantly ($p = 0.213$, Wilcoxon signed-rank test). These statistical values are better detailed in Table 2b.

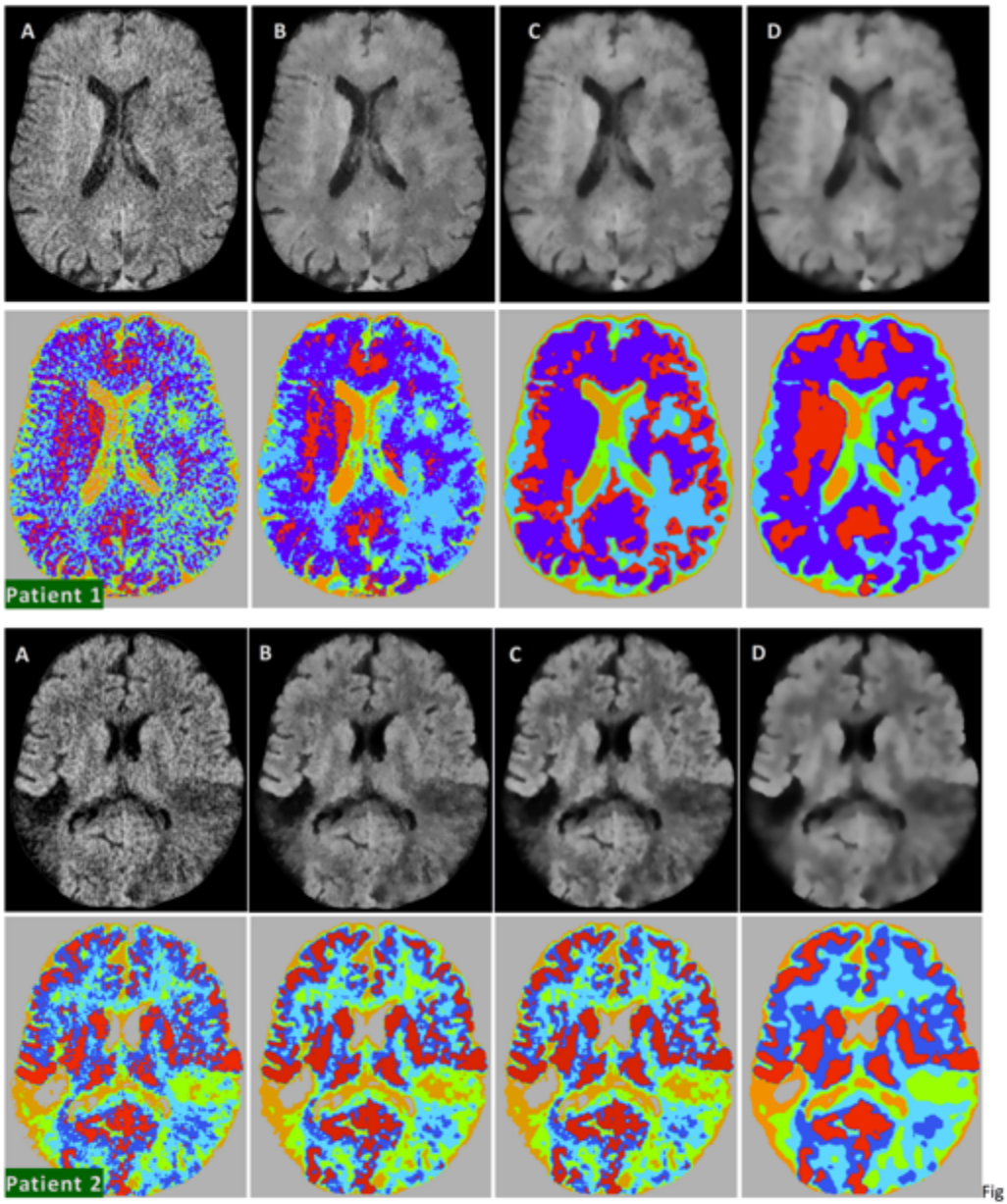

Fig 2a – Examples of results of each step of image treatment (first row), as well as its SOM Clustering (second row) for each step of filtering of infarct Patients (patient 1 and 2) – A, with CLAHE equalization; B – with CLAHE + SUSAN filters; C – with CLAHE + SUSAN + Anisotropic Diffusion (AD) filters; D – with CLAHE + SUSAN + AD + Bilateral filters

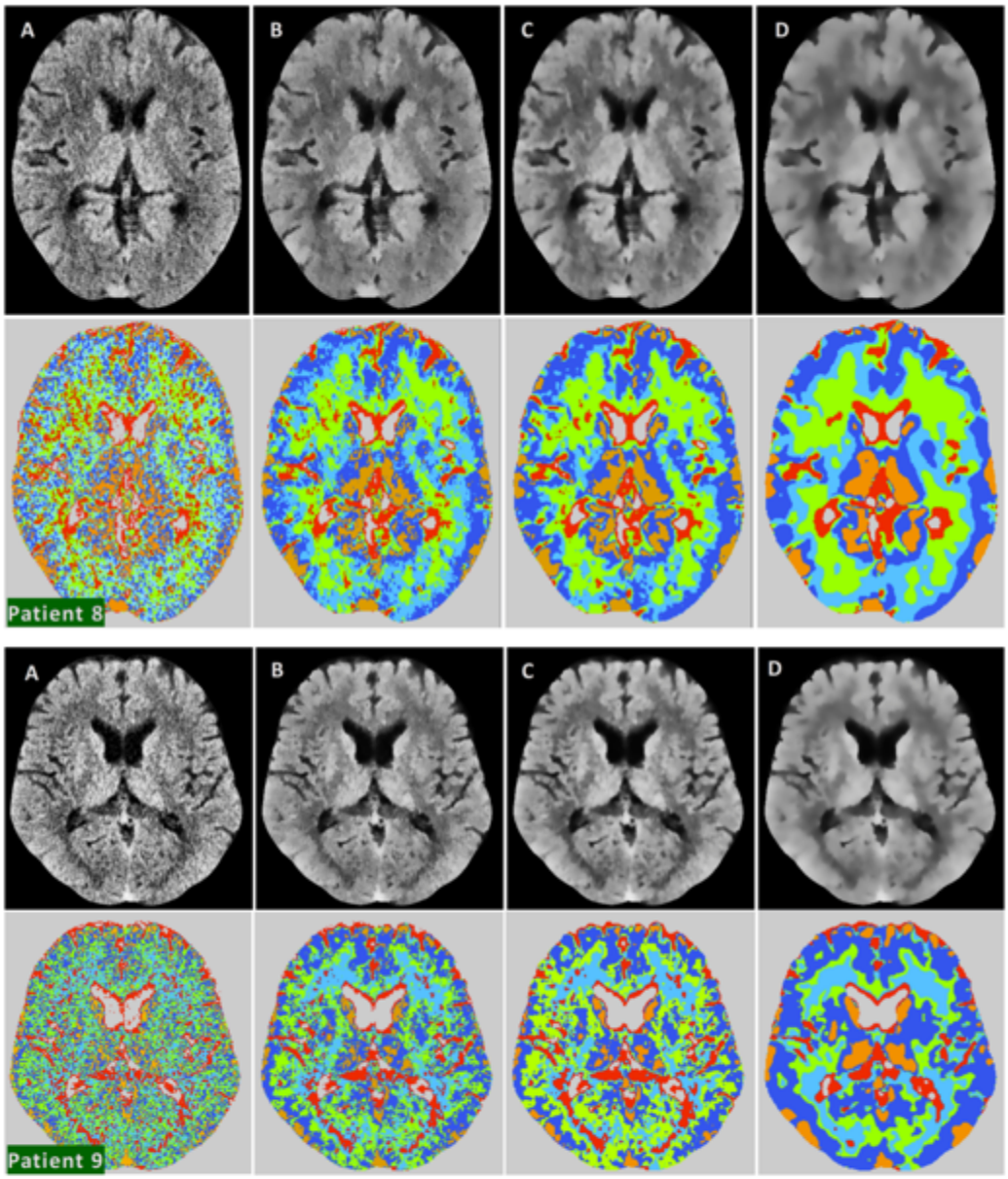

Fig 2b – Example of results of each step of image treatment (first row), as well as its SOM Clustering (second row) for each step of filtering of Patients with normal brain CTs (patient 8 and 9) – A, with CLAHE equalization; B – with CLAHE + SUSAN filters; C – with CLAHE + SUSAN + Anisotropic Diffusion (AD) filters; D – with CLAHE + SUSAN + AD + Bilateral filters

Patient	Infarct?	Asymmetrical (A) or Symmetrical (S)?					Interpretation	SSIM Index
		Rater 1	*Rater 2*	*Rater 3*	*Rater 4*	*Rater 5*		
1	Y	A	A	A	A	A	Asymmetrical	0.912
2	Y	A	S	A	A	A	Asymmetrical	0.915
3	Y	S	S	S	A	S	Symmetrical	0.938
4	Y	A	A	A	A	A	Asymmetrical	0.889
5	N	A	S	A	A	A	Asymmetrical	0.923
6	N	A	A	S	A	S	Asymmetrical	0.934
7	Y	A	S	A	A	S	Asymmetrical	0.939
8	Y	A	A	S	A	A	Asymmetrical	0.911
9	Y	A	A	A	S	A	Asymmetrical	0.895
10	Y	S	S	S	A	S	Symmetrical	0.919
11	Y	A	S	A	A	A	Asymmetrical	0.927
12	N	S	S	S	A	S	Symmetrical	0.935
13	Y	A	A	A	A	S	Asymmetrical	0.932
14	N	S	S	S	A	S	Symmetrical	0.931
15	N	S	S	S	S	S	Symmetrical	0.936
16	N	S	S	S	S	S	Symmetrical	0.935
17	N	S	A	S	S	S	Symmetrical	0.933
18	N	S	S	S	A	S	Symmetrical	0.866
19	N	S	A	A	A	S	Asymmetrical	0.940

Table 2a – Evaluation of asymmetry from independent examiners

	POSITIVE for Infarct	**NEGATIVE for Infarct**	
Asymmetrical	8	3	11
Symmetrical	2	6	8
	10	9	19
Sensitivity = 8/10 = 0.8 Specificity = 6/9 ≃ 0.67 Accuracy = 14/19 ≃ 0.74		Positive Predictive Value = 8/11 ≃ 0.73 Negative Predictive Value = 6/8 = 0.75	
Mean SSIM index	0.918	0.926	p = 0.213

Table 2b – Statistical values of the analyses

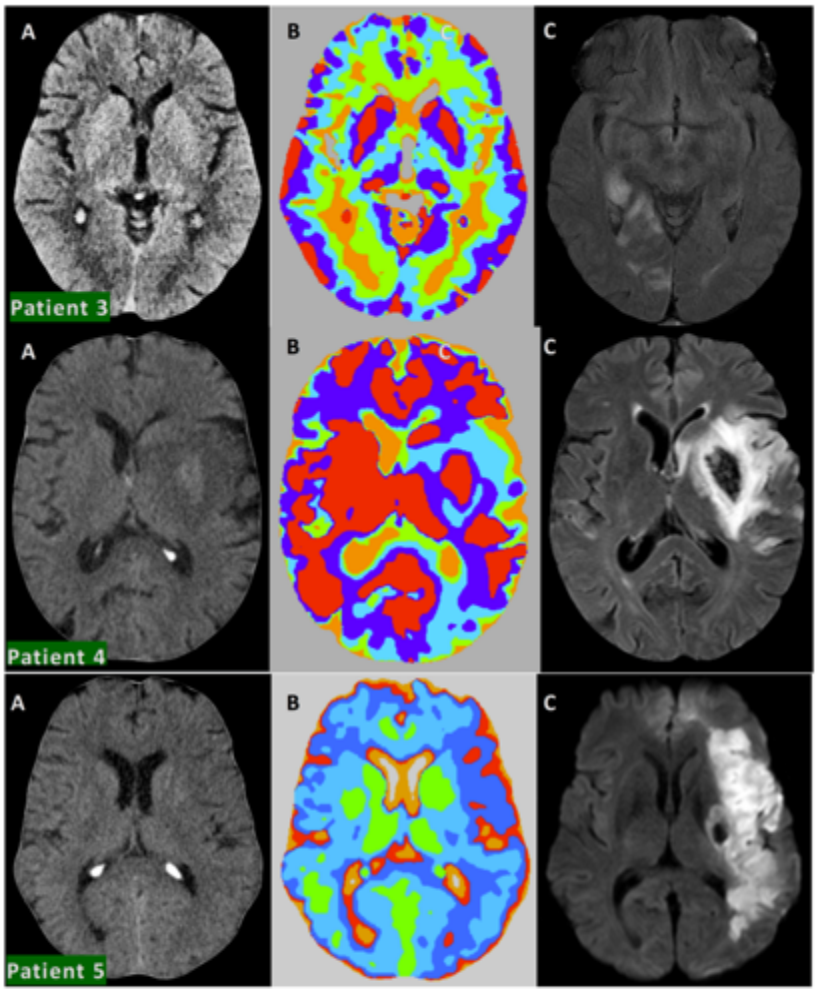

Fig. 3 - Stroke patients 3, 4 and 5, from left to right: A - original CT, B - clustering results after triple filtering and C - FLAIR MRI showing the infarct location

Discussion

For the majority of controls, the images were considered symmetrical by the majority of raters, that is, a symmetry of clustering assignment between the right and the left hemispheres could be better seen after the final round of filtering, with similar colors corresponding more or less to the same structures in each side. In infarct cases, patient 3, who had a right posterior cerebral artery infarct, did not show any differences between both hemispheres (fig. 3), indicating that the technique may not be accurate for the detection of all subtle or hyperacute infarctions.

The majority of examiners considered 08 out of 10 cases with infarct as having asymmetry of colors, as seen in patient 1 (fig. 2a), where the affected side had a substantial decrease of the red cluster as well as an increase of the light blue cluster, when compared to the healthy side. In patient 2 (also fig. 2a) with bilateral occipital infarcts the color that predominates in each side is different, reflecting infarcts of different age (old on the right and acute on the left), with old infarct showing predominance of orange color, and both the old and acute infarcts lacking red cluster. An area of hemorrhagic transformation in Patient 4 (fig. 3) was assigned the same cluster color as most of the normal right hemisphere.

Having sensitivity, accuracy and PPV equal to or higher than 70% indicates that clear visual asymmetry after SOM clustering on triple smoothing filtering was a relatively successful predictor of infarction in our database. On the contrary, a NPV lower than 70% demonstrates that symmetry was not a reliable indicator for lack of ischemia in the CNS.

The use of triple filtering provided better separation of clusters in comparison to images generated using less filtering steps. For example, in patient 1 (fig 2a), triple filtering made clustering less prone to spending one colored cluster in an unnecessary red halo bordering margins of an already assigned cluster, that happened in step C, but went away in step D (triple filtering). Also, in the same figure, patient 2 had nuances of orange that were previously on the left inferior quadrant gone away in step D, being orange then assigned only for pixels with lower intensities.

Conclusion

Image pre-processing is an important step for improving segmentation of brain CT images. Our work suggests that a combination of different smoothing filters does a better job than single filtering on avoiding grainy, heterogeneous clusters, and delivering smooth segments with continuous borders.

Even though the precision of segmentation remains worse than in MRI, where usually the clusters match more precisely the borders of different brain structures, and despite the lack of quantitative significant SSIM index of asymmetry, one may still have, with this method, a qualitative, visual cue to help the identification of brain lesions that may not be as obvious for a medical staff being only given the regular CT scan for evaluation.

Not all CTs positive for lesions showed asymmetry, but having sensitivity, PPV and NPV values above 70% suggests that SOM clustering after triple filtering may be a useful method to help the diagnosis. We believe, despite obtaining modest results concerning border precision with SOM segmentation, that the publication of our current data is important, given the fact that up to date there is, in contrast to available information on MRI, very little published data about automated segmentation on CT images, and more research on the matter should always be encouraged, once CT imaging has a much wider availability throughout the world, in comparison to MRI.

The identification of clear clustering asymmetry between hemispheres, through the use of multiple structure-preserving filtering can, therefore, provide help for identifying structural changes in CT scans. Given the fact that the image filtering and clustering proposed on this work do not require very powerful computer processing, and thus could be done promptly by a medical staff using an ordinary computer, or even a portable device, it could be very useful to recognize an area of ischemic brain damage. Therefore, further improvements of this combination of filters, as well as other combinations of pre-processing techniques should be encouraged on brain CT segmentation.

Acknowledgements

The authors would like to thank the Coordination for the Improvement of Higher Education Personnel – CAPES, Brazil, for providing financial support for the research.

References

1. Maldjian JA, Chalela J, Kasner SE, Liebeskind D, Detre JA. Automated CT segmentation and analysis for acute middle cerebral artery stroke. Am J Neuroradiol. 2001;22(6):1050–5.
2. Smith S, Brady J. SUSAN—a new approach to low level image processing. Int J Comput Vis [Internet]. 1997;23(1):45–78. Available from: http://link.springer.com/article/10.1023/A:1007963824710
3. Tomasi C, Manduchi R. Bilateral filtering for gray and color images. Sixth Int Conf Comput Vis (IEEE Cat No98CH36271) [Internet]. 1998;839–46. Available from: http://ieeexplore.ieee.org/document/710815/
4. Perona P, Malik J. Scale-space and edge detection using anisotropic diffusion. IEEE Trans Pattern Anal Mach Intell [Internet]. 1990;12(7):629–39. Available from: http://ieeexplore.ieee.org/lpdocs/epic03/wrapper.htm?arnumber=56205
5. Kohonen T. Self-organized formation of topologically correct feature maps. Biol Cybern [Internet]. 1982;43(1):59–69. Available from: http://link.springer.com/10.1007/BF00337288
6. Li Y, Chi Z. MR Brain Image Segmentation Based on Self-Organizing Map Network. Int J Inf Technol. 2005;11(8):45–53.
7. Vijayakumar C, Damayanti G, Pant R, Sreedhar CM. Segmentation and grading of brain tumors on apparent diffusion coefficient images using self-organizing maps. Comput Med Imaging Graph. 2007;31(7):473–84.
8. Mei PA, De Carvalho Carneiro C, Fraser SJ, Min LL, Reis F. Analysis of neoplastic lesions in magnetic resonance imaging using self-organizing maps. J Neurol Sci. 2015;359(1–2):78–83.
9. Mei PA, de Carvalho Carneiro C, Kuroda MC, Fraser SJ, Min LL, Reis F. Self-organizing maps as a tool for segmentation of Magnetic Resonance Imaging (MRI) of relapsing-remitting multiple sclerosis. In: Self-Organizing Maps and Learning Vector Quantization, Clustering and Data Visualization (WSOM), 2017 12th International Workshop on. IEEE; 2017. p. 1–7.
10. Pexman JHW, Barber PA, Hill MD, Sevick RJ, Demchuk AM, Hudon ME, et al. Use of the Alberta

Stroke Program Early CT Score (ASPECTS) for assessing CT scans in patients with acute stroke. Am J Neuroradiol. 2001;22(8):1534–42.

11. Hacke W, Kaste M, Bluhmki E, Brozman M, al et. (ECASS III)Thrombolysis with alteplase 3 to 4.5 hours after acute ischemic stroke. … Engl J … [Internet]. 2008; Available from: http://www.nejm.org/doi/full/10.1056/NEJMoa0804656%5Cnpapers3://publication/uuid/32D781E8-C673-4EDD-961E-9C21FF830518

12. Schindelin J, Arganda-Carreras I, Frise E, Kaynig V, Longair M, Pietzsch T, et al. Fiji: an open-source platform for biological-image analysis. Nat Methods [Internet]. 2012;9(7):676–82. Available from: http://www.ncbi.nlm.nih.gov/pubmed/22743772%0Ahttp://www.pubmedcentral.nih.gov/articlerender.fcgi?artid=PMC3855844

13. Schindelin J, Rueden CT, Hiner MC, Eliceiri KW. The ImageJ ecosystem: An open platform for biomedical image analysis. Vol. 82, Molecular Reproduction and Development. 2015. p. 518–29.

14. Zuiderveld K. Graphics Gems IV. In: Heckbert PS, editor. San Diego, CA, USA: Academic Press Professional, Inc.; 1994. p. 474–85. Available from: http://dl.acm.org/citation.cfm?id=180895.180940

15. ESRI ESRI. ArcGIS Desktop [Internet]. 2011. Available from: https://www.arcgis.com/

16. Frank E, Hall MA, Witten IH. The WEKA Workbench. Online Appendix for "Data Mining: Practical Machine Learning Tools and Techniques" Morgan Kaufmann, Fourth Ed. 2016;

17. Wang Z, Bovik AC, Sheikh HR, Simoncelli EP. Image quality assessment: from error visibility to structural similarity. IEEE Trans image Process. 2004;13(4):600–12.

5. DISCUSSÃO

5.1 Sobre o potencial geral de segmentação por SOM de neuroimagens médicas

5.1.1 RM

Os Artigos I e II demonstraram que, através da análise por SOM dos pixels de lesões neoplásicas e desmielinizantes, houve êxito bastante razoável na utilização desta ferramenta não-supervisionada em separar as porções acometidas por patologia do restante saudável do tecido nervoso.

5.1.2 TC

De modo oposto ao êxito em imagens de RM, a falta de delimitação mais precisa de lesões isquêmicas em TC por SOM, ao menos quando não há preparo/tratamento prévio robusto de imagens de TC, no Artigo III, embora algo frustrante e ao mesmo tempo esperado, evidencia que, possivelmente, uma maior exploração de pré-filtros de suavização e ajustes ou complementação por outras técnicas, possivelmente num misto de processos supervisionados + não-supervisionados, pode ser um caminho a ser desenvolvido para o aprimoramento de investigação de lesões em TC.

Esta investigação em TC, naturalmente. se mostra bem mais custosa quando se cobra precisão parecida com a RM, dado o fato das imagens da primeira terem resolução drasticamente menor que as da segunda.

5.2 Sobre o potencial do SOM específico a cada natureza de lesão estudada

5.2.1 Neoplasias (Artigo I)

O artigo I permitiu avaliar, além da capacidade de segmentação, as diferentes *assinaturas* de tumores de origem diferente, ie, se os valores de cinza em T1, T2 e FLAIR se encontravam baixos, médios ou altos em relação à média para cada tipo de tumor. Como exemplo: os Glioblastomas foram os únicos, entre todos os tumores, que apresentaram valores baixos de cinza

da lesão em T2. Da mesma forma, os Gangliogliomas apresentaram os valores de cinza das lesões mais baixos em FLAIR. Um aprofundamento do estudo de assinaturas das sequências de tumores, em estudos futuros, poderia ser uma ferramenta adicional a corroborar identificação não invasiva do tipo tumoral.

Também merece destaque a segmentação correta, em boa parte dos casos, das diferentes porções tumorais (ex: parte tumoral sólida vs parte necrótica-liquefativa vs edema perilesional) em diferentes clusters.

5.2.2 Esclerose Múltipla Remitente-Recorrente (Artigo II)

A técnica de SOM se mostrou razoavelmente precisa para separar lesões desmielinizantes de tecido sadio. Houve, contudo, alguma inclusão de tecido cortical no mesmo cluster das lesões, por provável similaridade de tons de cinza, embora deva-se cogitar a possibilidade de haver acometimento igualmente nesta região, uma vez que se sabe atualmente que também há comprometimento cortical/juxtacortical na EM. Não houve êxito quanto à diferenciação de lesões novas de antigas.

5.2.3 AVC Isquêmico (Artigo III)

Tendo como base as variáveis analisadas, os SOM não se mostraram capazes de segmentar com precisão e delineamento aceitáveis imagens de TC que não tivessem algum tratamento prévio, gerando imagens granuladas e sem coesão dos pixels. O pré-tratamento com filtros de suavização inteligente, ie, filtros que suavizam o tecido cerebral tentando não borrar as bordas corticais ou mesmo a transição entre parênquima e ventrículos, se mostrou eficaz em promover maior homogeneização dos clusters, contudo não houve ainda assim uma delimitação precisa de lesões vasculares recentes, o que já era esperado, dado o fato de, além da TC ter menor resolução que a RM, lesões recentes são de fato de difícil diagnóstico apenas pela interpretação da TC simples, sem complementação por outros métodos como TC de perfusão, angio-TC ou mesmo RM com sequências de difusão e perfusão.

Ainda assim, nota-se que na maioria dos casos em que houve de fato AVCi, havia, qualitativamente, uma percepção maior de assimetria entre ambos hemisférios ante aos controles. Um maior estudo de pré-filtros, aliados a uma possível combinação de diferentes redes neurais, possivelmente com etapas supervisionadas e não-supervisionadas (como SOM), poderia se mostrar útil futuramente.

5.3 Sobre a viabilidade do uso de técnicas de segmentação mais modestas (Não Deep-Learning) no cenário atual

Embora haja uma tendência crescente do uso de computadores complexos, com capacidade de calcular uma quantidade imensa de dados ("Very" Big Data), o êxito dos SOM, técnica comparativamente mais simples, uma vez que não há uso de supercomputador, em segmentar com sucesso a maioria das lesões dos pacientes submetidos a RM de neuropatologias (ie, Artigos I e II) mostra que ainda há espaço e viabilidade para o uso de técnicas mais modestas ou antigas de neurocomputação, como SOM, Árvores de Decisão, LVQ, K-Médias, etc.

6. CONCLUSÕES

- A análise de neuroimagens por SOM se mostrou opção viável para a segmentação com precisão aceitável para imagens de neoplasias e lesões desmielinizantes escaneadas em RM usadas nesta nesta pesquisa;

- Neoplasias de SNC em geral foram segmentadas corretamente, com razoável separação de porções tumorais diferentes (ex: parte tumoral sólida vs parte necrótica-liquefativa vs edema perilesional). Tumores de linhagens diferentes por vezes apresentaram *assinaturas* (explicação no item 5.2.1) distintas;

- Lesões desmielinizantes na Esclerose Múltipla forma Remitente-Recorrente foram nesta série bem separadas por SOM de tecido sadio, salvo alguma inclusão de tecido cortical no mesmo cluster, por similaridade de tons de cinza, porém sem clareza quanto à existência de lesão neste; não houve sucesso em diferenciação de lesões novas vs antigas;

- O potencial de SOM e da maioria das NN disponíveis atualmente (mais antigas e mais novas), para imagens de TC, permanece ainda uma incógnita, uma vez que para a primeira ainda há maior escassez de informações que para imagens de RM e um grau elevado de incertezas quanto à melhor metodologia a ser aplicada, bem como quais filtros (suavização e outros) poderiam ser empregados previamente à segmentação.

7. REFERÊNCIAS

1. Wiener N. Cybernetics. Sci Am. 1948;179:14–8.
2. Nordbotten S. Automatic Files in Statistical Systems. Statistical Standarts and Studies. 1967.
3. Yang J, Huang T. Image super-resolution: Historical overview and future challenges. Super-resolution imaging. CRC Press; 2010;20–34.
4. McCarthy J, Minsky ML, Rochester N, Shannon CE. A Proposal for the Dartmouth Summer Research Project on Artificial Intelligence, August 31, 1955. AI Mag [Internet]. 2006;27(4):12. Available from: http://www.aaai.org/ojs/index.php/aimagazine/article/view/1904
5. Schank RC. Where's The AI ? AI Mag. 1991;12(4):38–50.
6. Blog Nv. What's the Difference Between Artificial Intelligence, Machine Learning, and Deep Learning? [Internet]. [cited 2018 Jan 16]. Available from: https://blogs.nvidia.com/blog/2016/07/29/whats-difference-artificial-intelligence-machine-learning-deep-learning-ai/
7. Lent R. Cem Bilhões de Neurônios? 2nd ed. Atheneu; 2010. 786 p.
8. Nordbotten S. Data Mining with Neural Networks [Internet]. 2006. Available from: http://nordbotten.com/articles/NN.pdf
9. McCulloch WS, Pitts W. A logical calculus of the ideas immanent in nervous activity. Bull Math Biophys. Springer; 1943;5(4):115–33.
10. Rosenblatt F. The perceptron: a probabilistic model for information storage and organization in the brain. Psychol Rev. 1958;65(6):386–408.
11. Le Cun Y. Une procedure d'apprentissage pour reseau a seuil assymetrique (A learning procedure for assymetric threshold networks). In: Proceedings of Cognitiva 85. 1985. p. 599–604 ST.
12. Parker DB. Learning-Logic: Casting the Cortex of the Human Brain in Silicon. Vol. TR-47. Cambridge, MA; 1985.
13. Rumelhart DE, McClelland JL, Group PDPR. Parallel Distributed Pocessing. IEEE. IEEE; 1988;1:443–53.
14. Minsky ML. Computation: Finite and Infinite Machines. Prentice-Hall, Inc.; 1967. 317 p.
15. Alexander I. Neural Computing Architectures: The Design of Brain-like Machines. Vol. 1. North Oxford Academic Publishing Co Ltd; 1989.
16. Hecht-Nielsen R. Neurocomputing. Addison-Wesley; 1990. 433 p.
17. Bishop CM. Neural networks for pattern recognition. Oxford university press; 1995. 504 p.
18. van Veen F, Asimov Institute. The Neural Network Zoo [Internet]. 2016 [cited

2017 Mar 29]. Available from: http://www.asimovinstitute.org/neural-network-zoo/

19. Kohonen T. Data Management by Self Organizing Maps [Internet]. 2014 [cited 2017 Jun 6]. Available from: https://www.youtube.com/watch?v=iWPhGKniTew&t=634s

20. Sjöberg M, Laaksonen J. Optimal combination of som search in best-matching units and map neighborhood. In: International Workshop on Self-Organizing Maps. Springer; 2009. p. 281–9.

21. Ultsch A. U*-matrix: a tool to visualize clusters in high dimensional data [Internet]. Fachbereich Mathematik und Informatik Marburg; 2003. Available from: https://pdfs.semanticscholar.org/1d9d/ba44f2d237ee9d8f0388299afbcc0e581621.pdf

22. Borghi M, Maggiolino M, Montagnani M, Nuccio M. Determinants in the online distribution of digital content: An exploratory analysis. Vol. 3, European Journal of Law and Technology. 2012.

23. Gan G, Ma C, Wu J. Data Clustering: Theory, Algorithms, and Applications. ASASIAM Series on Statistics and Applied. 2007. 466 p.

24. Berkhin P. A survey of clustering data mining techniques. In: Grouping multidimensional data. Springer; 2006. p. 25–71.

25. Johansen AR, Jin J, Maszczyk T, Dauwels J, Cash SS, Westover MB. Epileptiform spike detection via convolutional neural networks. In: Acoustics, Speech and Signal Processing (ICASSP), 2016 IEEE International Conference on. IEEE; 2016. p. 754–8.

26. Acharya UR, Oh SL, Hagiwara Y, Tan JH, Adeli H. Deep convolutional neural network for the automated detection and diagnosis of seizure using EEG signals. Comput Biol Med. Elsevier; 2017;

27. Oropesa E, Cycon HL, Jobert M. Sleep stage classification using wavelet transform and neural network. Int Comput Sci Inst. 1999;

28. Shimada T, Shiina T, Saito Y. Detection of characteristic waves of sleep EEG by neural network analysis. IEEE Trans Biomed Eng. IEEE; 2000;47(3):369–79.

29. van Putten MJAM, Olbrich S, Arns M. Predicting sex from brain rhythms with deep learning. Sci Rep. England; 2018 Feb;8(1):3069.

30. Wu D, Warwick K, Ma Z, Gasson MN, Burgess JG, Pan S, et al. Prediction of Parkinson's disease tremor onset using a radial basis function neural network based on particle swarm optimization. Int J Neural Syst. World Scientific; 2010;20(2):109–16.

31. Suzuki K. Overview of deep learning in medical imaging. Radiol Phys Technol. Japan; 2017 Sep;10(3):257–73.

32. Esposito F, Scarabino T, Hyvarinen A, Himberg J, Formisano E, Comani S, et al. Independent component analysis of fMRI group studies by self-organizing clustering. Neuroimage. Elsevier; 2005;25(1):193–205.

33. Peltier SJ, Polk TA, Noll DC. Detecting low-frequency functional connectivity in fMRI using a self-organizing map (SOM) algorithm. Hum Brain Mapp. Wiley Online Library; 2003;20(4):220–6.

34. ESRI ESRI. ArcGIS Desktop [Internet]. 2011. Available from: https://www.arcgis.com/

35. CSIRO. SiroSOM [Internet]. Queensland: CSIRO Australia; Available from: https://www.csiro.au/en/Research/MRF/Areas/Mining-and-mining-systems/Intelligent-mining/Self-organising-maps

36. Frank E, Hall MA, Witten IH. The WEKA Workbench. Online Appendix for "Data Mining: Practical Machine Learning Tools and Techniques." 4th ed. Morgan Kaufmann; 2016. 128 p.

37. Davies DL, Bouldin DW. A cluster separation measure. IEEE Trans Pattern Anal Mach Intell. IEEE; 1979;(2):224–7

8. ANEXOS

8.1 Parecer Consubstanciado do Comitê de Ética em Pesquisa

FACULDADE DE CIENCIAS MEDICAS - UNICAMP (CAMPUS CAMPINAS)

PARECER CONSUBSTANCIADO DO CEP

DADOS DO PROJETO DE PESQUISA

Título da Pesquisa: ANÁLISE DE LESÕES TUMEFATIVAS EM RESSONÂNCIA MAGNÉTICA A PARTIR DE MAPAS AUTO-ORGANIZÁVEIS

Pesquisador: Paulo Afonso Mei

Área Temática:

Versão: 1

CAAE: 06894012.8.0000.5404

Instituição Proponente: Hospital de Clínicas - UNICAMP

DADOS DO PARECER

Número do Parecer: 130.280

Data da Relatoria: 23/10/2012

Apresentação do Projeto:

O estudo consistirá na análise por software de mapas auto-organizáveis de imagens de ressonância magnética do encéfalo obtidas em ponderações T1, FLAIR e T2, com ou sem contraste, a fim de obter nova imagem separada por clusters semelhantes.

Objetivo da Pesquisa:

Determinações mais precisas da natureza de lesões tumefativas baseados em análises retrospectivas automáticas obtidas através do SOM, correlacionando esses achados com os diagnósticos clínicos retrospectivos definitivos (biópsias ou exame subsidiário que corrobore o diagnóstico).

Avaliação dos Riscos e Benefícios:

Não há risco para os sujeitos, uma vez que o estudo será realizado analisando imagens de RM do encéfalo já existentes. O estudo poderá oferecer futuramente possível ferramenta não invasiva adicional no diagnóstico neuroimagenológico.

Comentários e Considerações sobre a Pesquisa:

A pesquisa está bem estruturada e metodologia bem definida.

Considerações sobre os Termos de apresentação obrigatória:

Solicitou dispensa do TCL com justificativa adequada.

Recomendações:

-

Endereço: Rua Tessália Vieira de Camargo, 126
Bairro: Barão Geraldo **CEP:** 13.083-887
UF: SP **Município:** CAMPINAS
Telefone: (19)3521-8936 **Fax:** (19)3521-7187 **E-mail:** cep@fcm.unicamp.br

FACULDADE DE CIENCIAS MEDICAS - UNICAMP (CAMPUS CAMPINAS)

Conclusões ou Pendências e Lista de Inadequações:

A pesquisa está bem estruturada e metodologia bem definida. Aprovado com dispensa do TCLE.

Situação do Parecer:

Aprovado

Necessita Apreciação da CONEP:

Não

Considerações Finais a critério do CEP:

CAMPINAS, 24 de Outubro de 2012

Assinador por:
Carlos Eduardo Steiner
(Coordenador)

Endereço: Rua Tessália Vieira de Camargo, 126
Bairro: Barão Geraldo **CEP:** 13.083-887
UF: SP **Município:** CAMPINAS
Telefone: (19)3521-8936 **Fax:** (19)3521-7187 **E-mail:** cep@fcm.unicamp.br

8.2 Permissões de republicação dos artigos

8.2.1 Artigo I

must be made, either as a footnote or in a reference list at the end of your publication, as follows:

"Reprinted from Publication title, Vol /edition number, Author(s), Title of article / title of chapter, Pages No., Copyright (Year), with permission from Elsevier [OR APPLICABLE SOCIETY COPYRIGHT OWNER]." Also Lancet special credit - "Reprinted from The Lancet, Vol. number, Author(s), Title of article, Pages No., Copyright (Year), with permission from Elsevier."

4. Reproduction of this material is confined to the purpose and/or media for which permission is hereby given.

5. Altering/Modifying Material: Not Permitted. However figures and illustrations may be altered/adapted minimally to serve your work. Any other abbreviations, additions, deletions and/or any other alterations shall be made only with prior written authorization of Elsevier Ltd. (Please contact Elsevier at permissions@elsevier.com). No modifications can be made to any Lancet figures/tables and they must be reproduced in full.

6. If the permission fee for the requested use of our material is waived in this instance, please be advised that your future requests for Elsevier materials may attract a fee.

7. Reservation of Rights: Publisher reserves all rights not specifically granted in the combination of (i) the license details provided by you and accepted in the course of this licensing transaction, (ii) these terms and conditions and (iii) CCC's Billing and Payment terms and conditions.

8. License Contingent Upon Payment: While you may exercise the rights licensed immediately upon issuance of the license at the end of the licensing process for the transaction, provided that you have disclosed complete and accurate details of your proposed use, no license is finally effective unless and until full payment is received from you (either by publisher or by CCC) as provided in CCC's Billing and Payment terms and conditions. If full payment is not received on a timely basis, then any license preliminarily granted shall be deemed automatically revoked and shall be void as if never granted. Further, in the event that you breach any of these terms and conditions or any of CCC's Billing and Payment terms and conditions, the license is automatically revoked and shall be void as if never granted. Use of materials as described in a revoked license, as well as any use of the materials beyond the scope of an unrevoked license, may constitute copyright infringement and publisher reserves the right to take any and all action to protect its copyright in the materials.

9. Warranties: Publisher makes no representations or warranties with respect to the licensed material.

10. Indemnity: You hereby indemnify and agree to hold harmless publisher and CCC, and their respective officers, directors, employees and agents, from and against any and all claims arising out of your use of the licensed material other than as specifically authorized pursuant to this license.

11. No Transfer of License: This license is personal to you and may not be sublicensed, assigned, or transferred by you to any other person without publisher's written permission.

12. No Amendment Except in Writing: This license may not be amended except in a writing signed by both parties (or, in the case of publisher, by CCC on publisher's behalf).

13. Objection to Contrary Terms: Publisher hereby objects to any terms contained in any purchase order, acknowledgment, check endorsement or other writing prepared by you, which terms are inconsistent with these terms and conditions or CCC's Billing and Payment terms and conditions. These terms and conditions, together with CCC's Billing and Payment terms and conditions (which are incorporated herein), comprise the entire agreement between you and publisher (and CCC) concerning this licensing transaction. In the event of any conflict between your obligations established by these terms and conditions and those established by CCC's Billing and Payment terms and conditions, these terms and conditions shall control.

14. Revocation: Elsevier or Copyright Clearance Center may deny the permissions described in this License at their sole discretion, for any reason or no reason, with a full refund payable to you. Notice of such denial will be made using the contact information provided by you. Failure to receive such notice will not alter or invalidate the denial. In no event will Elsevier or Copyright Clearance Center be responsible or liable for any costs, expenses or damage incurred by you as a result of a denial of your permission request, other than a refund of the amount(s) paid by you to Elsevier and/or Copyright Clearance Center for denied permissions.

LIMITED LICENSE

The following terms and conditions apply only to specific license types:

15. **Translation**: This permission is granted for non-exclusive world **English** rights only unless your license was granted for translation rights. If you licensed translation rights you may only translate this content into the languages you requested. A professional translator must perform all translations and reproduce the content word for word preserving the integrity of the article.

16. **Posting licensed content on any Website**: The following terms and conditions apply as follows: Licensing material from an Elsevier journal: All content posted to the web site must maintain the copyright information line on the bottom of each image; A hyper-text must be included to the Homepage of the journal from which you are licensing at http://www.sciencedirect.com/science/journal/xxxxx or the Elsevier homepage for books at

http://www.elsevier.com; Central Storage: This license does not include permission for a scanned version of the material to be stored in a central repository such as that provided by Heron/XanEdu.
Licensing material from an Elsevier book: A hyper-text link must be included to the Elsevier homepage at http://www.elsevier.com . All content posted to the web site must maintain the copyright information line on the bottom of each image.

Posting licensed content on Electronic reserve: In addition to the above the following clauses are applicable: The web site must be password-protected and made available only to

bona fide students registered on a relevant course. This permission is granted for 1 year only. You may obtain a new license for future website posting.
17. **For journal authors:** the following clauses are applicable in addition to the above:
Preprints:
A preprint is an author's own write-up of research results and analysis, it has not been peer-reviewed, nor has it had any other value added to it by a publisher (such as formatting, copyright, technical enhancement etc.).
Authors can share their preprints anywhere at any time. Preprints should not be added to or enhanced in any way in order to appear more like, or to substitute for, the final versions of articles however authors can update their preprints on arXiv or RePEc with their Accepted Author Manuscript (see below).
If accepted for publication, we encourage authors to link from the preprint to their formal publication via its DOI. Millions of researchers have access to the formal publications on ScienceDirect, and so links will help users to find, access, cite and use the best available version. Please note that Cell Press, The Lancet and some society-owned have different preprint policies. Information on these policies is available on the journal homepage.
Accepted Author Manuscripts: An accepted author manuscript is the manuscript of an article that has been accepted for publication and which typically includes author-incorporated changes suggested during submission, peer review and editor-author communications.
Authors can share their accepted author manuscript:

- immediately
  - via their non-commercial person homepage or blog
  - by updating a preprint in arXiv or RePEc with the accepted manuscript
  - via their research institute or institutional repository for internal institutional uses or as part of an invitation-only research collaboration work-group
  - directly by providing copies to their students or to research collaborators for their personal use
  - for private scholarly sharing as part of an invitation-only work group on commercial sites with which Elsevier has an agreement
- After the embargo period
  - via non-commercial hosting platforms such as their institutional repository
  - via commercial sites with which Elsevier has an agreement

In all cases accepted manuscripts should:

- link to the formal publication via its DOI
- bear a CC-BY-NC-ND license - this is easy to do
- if aggregated with other manuscripts, for example in a repository or other site, be shared in alignment with our hosting policy not be added to or enhanced in any way to appear more like, or to substitute for, the published journal article.

Published journal article (JPA): A published journal article (PJA) is the definitive final record of published research that appears or will appear in the journal and embodies all value-adding publishing activities including peer review co-ordination, copy-editing, formatting, (if relevant) pagination and online enrichment.
Policies for sharing publishing journal articles differ for subscription and gold open access articles:
Subscription Articles: If you are an author, please share a link to your article rather than the full-text. Millions of researchers have access to the formal publications on ScienceDirect, and so links will help your users to find, access, cite, and use the best available version.

Theses and dissertations which contain embedded PJAs as part of the formal submission can be posted publicly by the awarding institution with DOI links back to the formal publications on ScienceDirect.
If you are affiliated with a library that subscribes to ScienceDirect you have additional private sharing rights for others' research accessed under that agreement. This includes use for classroom teaching and internal training at the institution (including use in course packs and courseware programs), and inclusion of the article for grant funding purposes.
Gold Open Access Articles: May be shared according to the author-selected end-user license and should contain a CrossMark logo, the end user license, and a DOI link to the formal publication on ScienceDirect.
Please refer to Elsevier's posting policy for further information.
18. **For book authors** the following clauses are applicable in addition to the above:

18. **For book authors** the following clauses are applicable in addition to the above:
Authors are permitted to place a brief summary of their work online only. You are not allowed to download and post the published electronic version of your chapter, nor may you scan the printed edition to create an electronic version. **Posting to a repository:** Authors are permitted to post a summary of their chapter only in their institution's repository.
19. **Thesis/Dissertation**: If your license is for use in a thesis/dissertation your thesis may be submitted to your institution in either print or electronic form. Should your thesis be published commercially, please reapply for permission. These requirements include permission for the Library and Archives of Canada to supply single copies, on demand, of the complete thesis and include permission for Proquest/UMI to supply single copies, on demand, of the complete thesis. Should your thesis be published commercially, please reapply for permission. Theses and dissertations which contain embedded PJAs as part of the formal submission can be posted publicly by the awarding institution with DOI links back to the formal publications on ScienceDirect.

Elsevier Open Access Terms and Conditions
You can publish open access with Elsevier in hundreds of open access journals or in nearly 2000 established subscription journals that support open access publishing. Permitted third party re-use of these open access articles is defined by the author's choice of Creative Commons user license. See our open access license policy for more information.
Terms & Conditions applicable to all Open Access articles published with Elsevier:
Any reuse of the article must not represent the author as endorsing the adaptation of the article nor should the article be modified in such a way as to damage the author's honour or reputation. If any changes have been made, such changes must be clearly indicated.
The author(s) must be appropriately credited and we ask that you include the end user license and a DOI link to the formal publication on ScienceDirect.
If any part of the material to be used (for example, figures) has appeared in our publication with credit or acknowledgement to another source it is the responsibility of the user to ensure their reuse complies with the terms and conditions determined by the rights holder.
Additional Terms & Conditions applicable to each Creative Commons user license:
CC BY: The CC-BY license allows users to copy, to create extracts, abstracts and new works from the Article, to alter and revise the Article and to make commercial use of the Article (including reuse and/or resale of the Article by commercial entities), provided the user gives appropriate credit (with a link to the formal publication through the relevant DOI), provides a link to the license, indicates if changes were made and the licensor is not represented as endorsing the use made of the work. The full details of the license are available at http://creativecommons.org/licenses/by/4.0.
CC BY NC SA: The CC BY-NC-SA license allows users to copy, to create extracts, abstracts and new works from the Article, to alter and revise the Article, provided this is not done for commercial purposes, and that the user gives appropriate credit (with a link to the formal publication through the relevant DOI), provides a link to the license, indicates if changes were made and the licensor is not represented as endorsing the use made of the work. Further, any new works must be made available on the same conditions. The full details of the license are available at http://creativecommons.org/licenses/by-nc-sa/4.0.
CC BY NC ND: The CC BY-NC-ND license allows users to copy and distribute the Article, provided this is not done for commercial purposes and further does not permit distribution of the Article if it is changed or edited in any way, and provided the user gives appropriate credit (with a link to the formal publication through the relevant DOI), provides a link to the license, and that the licensor is not represented as endorsing the use made of the work. The full details of the license are available at http://creativecommons.org/licenses/by-nc-nd/4.0.
Any commercial reuse of Open Access articles published with a CC BY NC SA or CC BY NC ND license requires permission from Elsevier and will be subject to a fee.
Commercial reuse includes:

- Associating advertising with the full text of the Article
- Charging fees for document delivery or access
- Article aggregation
- Systematic distribution via e-mail lists or share buttons

Posting or linking by commercial companies for use by customers of those companies.

20. **Other Conditions**:

v1.9

Questions? customercare@copyright.com or +1-855-239-3415 (toll free in the US) or +1-978-646-2777.

8.2.2 Artigo II